daf-16/FOXO promotes the activity of ligand-bound DAF-12/NHR to coordinate dauer recovery and post-dauer seam cell fate

Matthew J. Wirick[1], Isaac T. Smith[2], Benjamin S. Olson[2], Amelia F. Alessi[3], Himani Galagali[3], Kyal Lalk[2], Mikayla N. Schmidt[2], Kevin J. Ranke[2], John K. Kim[3], Xantha Karp[1,2,†]

1. Central Michigan University, Biochemistry, Cell & Molecular Biology Program
2. Central Michigan University, Department of Biology
3. Johns Hopkins University, Department of Biology

† Correspondence: karp1x@cmich.edu

Abstract

The mechanisms by which developmental pathways are modulated to accommodate developmental arrest are poorly understood. In adverse environments, dauer diapause can interrupt developmental progression after the second larval molt. During continuous (non-dauer) development, a heterochronic molecular timer consisting primarily of microRNAs and their targets controls the progression of stage-specific cell fates in lateral hypodermal seam cells. In unfavorable conditions, the DAF-16/FOXO transcription factor and the DAF-12 nuclear hormone receptor in its ligand-free state promote dauer formation and oppose the expression of *let-7* family microRNAs, thus pausing developmental progression during dauer. Surprisingly, we found that *daf-16(0)* post-dauer adults showed reiterative heterochronic defects including missing or gapped adult alae, lack of seam-cell fusion, and reduced expression of the adult-specific *col-19p::gfp* marker. Consistent with these adult cell fate defects, *let-7*-family microRNA expression was reduced in *daf-16(0)* post-dauer larvae. Addition of the DAF-12 ligand, dafachronic acid, suppressed the reiterative phenotypes in *daf-16(0)* post-dauer animals. Notably, addition of dafachronic acid to *daf-16* mutants rescued levels of *let-7* family transcriptional reporters but did not affect levels of these reporters in *daf-16(+)* control strains. Dafachronic acid is synthesized from cholesterol which is normally sequestered in the intestinal lumen during dauer. We found that a fluorescent cholesterol analog was not maintained in *daf-16* mutant larvae during dauer recovery. Consistent with this finding, timed auxin-mediated depletion of DAF-16 indicated that *daf-16* is required before dauer formation, rather than after dauer, to prevent reiterative seam cell fates in post-dauer larvae and adults. Furthermore, depletion of DAF-16 from the intestine recapitulated defects in adult cell fate. Taken together, we propose a model whereby *daf-16* acts prior to dauer formation to enable dafachronic acid synthesis by retaining cholesterol during dauer recovery. Ligand-bound DAF-12 then promotes dauer recovery and expression of *let-7* family microRNAs, thereby promoting adult cell fate. Thus, *daf-16* and *daf-12* coordinate dauer exit with the resumption of a developmental pathway.

Introduction

In a variety of species from nematodes to fish and insects, organisms can arrest their development into a stage termed “diapause” in response to or anticipation of adverse environmental conditions (Hand et al. 2016; Karp 2021). The underlying mechanisms that allow development to accommodate periods of developmental arrest and successfully attain proper developmental outcomes are less well understood. *Caenorhabditis elegans* larvae can either develop continuously or through a life history that includes dauer, a diapause stage. Dauer is a stress-resistant state occurring after the second larval molt, where the divisions of stem cell-like progenitor cells are halted (Cassada and Russell 1975; Hong et al. 1998). Favorable environmental conditions such as low population density, ambient temperatures, and abundant food sources promote TGFß and insulin/IGF-1 signaling (IIS) pathways. These pathways inhibit the activity of downstream transcription factors DAF-3/SMAD and DAF-16/FOXO, thus relieving negative regulation of DAF-9/CYTP450 that catalyzes the formation of dafachronic acid (DA), the ligand for the DAF-12 nuclear hormone receptor (NHR) (Fielenbach and Antebi 2008). Liganded DAF-12 promotes continuous development through the four larval stages (L1-L4), each separated by a molt, before reaching reproductive adulthood. If the environmental conditions are instead adverse, DAF-3/SMAD and DAF-16/FOXO are active and inhibit DAF-9/CYTP450 expression, preventing the biosynthesis of DA. The repressive, ligand-free form of DAF-12/NHR drives dauer formation (Antebi et al. 1998; Fielenbach and Antebi 2008; Baugh and Hu 2020). If dauer larvae find improved environmental conditions, they will undergo DAF-16/FOXO and DAF-12/NHR-dependent dauer recovery and resume development as post-dauer animals (Cassada and Russell 1975; Chen and Riddle 2008; Zhang and Sternberg 2022). In particular, the liganded form of DAF-12 is required for dauer exit. The production of DA depends on the availability of cholesterol which is sequestered in the intestinal lumen during dauer and then released during dauer recovery (Zhang and Sternberg 2022; Schmeisser et al. 2024).

Lateral hypodermal seam cells are a well-characterized model system that can be used to study the impact of dauer arrest on development (Sulston and Horvitz 1977; Liu and Ambros 1991). Seam cells are multipotent progenitor cells that undergo self-renewing divisions at least once each larval stage and then differentiate in adulthood (Sulston and Horvitz 1977). Characteristics of this differentiated adult cell fate include the permanent exit from the cell cycle, fusion of adjacent seam cells, expression of adult-enriched collagens, and the expression of adult-specific alae (Sulston and Horvitz 1977; Ambros and Horvitz 1984; Podbilewicz and White 1994; Liu et al. 1995). Stage-specific seam cell divisions and the onset of adult cell fate are

regulated through a network of heterochronic genes that encode transcription factors, RNA-binding proteins and microRNAs (miRNAs) (Ambros and Horvitz 1984; Rougvie and Moss 2013). The LIN-29 transcription factor is the most downstream heterochronic protein to promote adult cell fate and is expressed in the hypodermis of late L4 larvae (Ambros 1989; Bettinger et al. 1996; Azzi et al. 2020). Earlier in development, hypodermal LIN-29 expression is repressed by *lin-41* and *hbl-1* (Azzi et al. 2020). As development proceeds, the *let-7*-family miRNAs directly target *lin-41* and *hbl-1,* thus promoting LIN-29 expression and adult cell fate (Reinhart et al. 2000; Slack et al. 2000; Abrahante et al. 2003; Abbott et al. 2005; Azzi et al. 2020). The expression of the *let-7*-family miRNAs is regulated by DAF-12. In its liganded form, DAF-12-DA transcriptionally activates expression of the *let-7*-family miRNAs. In its ligand-free form, DAF-12 binds the DIN-1S corepressor to transcriptionally repress these miRNAs (Antebi et al. 1998; Ludewig et al. 2004; Motola et al. 2006; Bethke et al. 2009; Hammell et al. 2009).

The role of heterochronic genes in regulating stage-specific seam cell programs and the timing of the switch to adult cell fate has been studied primarily during continuous development (Ambros and Horvitz 1984). The dauer life history presents challenges to the timing of seam cell fates. During dauer, developmental progression must be halted indefinitely. After dauer, recovery from dauer arrest must be coordinated with the resumption of developmental programs. Perhaps for these reasons, the heterochronic gene network is altered during dauer, such that some heterochronic genes are required only during continuous development, whereas other aspects of the pathway are modulated in the dauer life history (Liu and Ambros 1991; Abrahante et al. 2003; Karp and Ambros 2012; Ilbay and Ambros 2019). The mechanisms by which the dauer formation pathway intersects with the heterochronic pathway to coordinate dauer diapause and recovery with the arrest and resumption of stage-specific cell fate specification are still incompletely understood. As described above, DAF-12 regulates both dauer formation and expression of the *let-7*-family miRNAs, creating a feedback loop that coordinates dauer formation and developmental arrest during dauer diapause (Hammell et al. 2009). In addition, the DAF-16 transcription factor promotes dauer formation and opposes adult cell fate during dauer through positive regulation of *lin-41* (Wirick et al. 2021). However, the role of the dauer formation genes in modulating developmental pathways during dauer recovery has not been described.

Here, we show that *daf-16* coordinates dauer exit and the resumption of seam cell development. We find that *daf-16* is required for the expression of multiple markers of adult cell fate in post-dauer adults, and for the transcription of the *let-7*-family miRNAs in post-dauer

larvae. These phenotypes in *daf-16* mutant post-dauer larvae are correlated with a delay in recovery from dauer. Remarkably, *daf-16* appears to act non-cell autonomously and prior to dauer formation to promote post-dauer adult cell fate. Addition of DA to recovering dauer larvae suppressed the dauer recovery, adult cell fate, and *let-7*-family expression phenotypes, suggesting that *daf-16* promotes activity of the ligand-bound form of DAF-12. We propose a model whereby *daf-16* promotes the expression of genes required for cholesterol sequestration. As dauer larvae recover, the cholesterol is converted to DA which then binds to DAF-12. The liganded DAF-12-DA complex promotes dauer recovery and transcription of the *let-7*-family miRNAs, coordinating the decision to exit dauer with the resumption of developmental programs.

Results

daf-16 promotes post-dauer adult cell fate and dauer recovery

We have previously shown that *daf-16* is required to prevent ectopic expression of an adult cell fate marker, *col-19p::gfp*, in hypodermal cells during dauer (Wirick et al. 2021). Since this adult marker was expressed in dauer larvae lacking *daf-16 (daf-16(0))* at high penetrance, we asked if the expression *of col-19p::gfp* persisted as larvae exited dauer and resumed development as post-dauer (PD) animals. To obtain dauer larvae in the dauer-defective *daf-16(0)* mutants, we used a temperature sensitive *daf-7(e1372ts)* allele that drives dauer formation when larvae are grown at 24-25°C (Vowels and Thomas 1992; Ogg et al. 1997). The *daf-7(e1327ts)* allele was present in the background of all strains that developed through the dauer life history in this study and for simplicity is not always mentioned. To induce recovery from dauer, dauer larvae were picked to new plates and shifted to 20°C. We found that the penetrance of *col-19p::gfp* expression was greatly reduced in PD *daf-16(0)* dauer larvae compared to the nearly complete penetrance observed during dauer (Figure 1A). Surprisingly, this marker remained largely off in PD adults (Figure 1A). By contrast, control *daf-16(+)* PD animals expressed *col-19p::gfp* at adulthood but not during PD larval stages, as expected (Figure 1A). Consistent with the reduced expression of an adult cell fate marker, we found that *daf-16(0)* PD animals failed to downregulate an L4 fate marker, *col-38p::yfp,* in adulthood (Figure S1) (Jackson et al. 2014). We have previously shown that *daf-16(0)* mutants that developed continuously, without dauer arrest, express *col-19p::gfp* normally, i.e., in adulthood but not larval stages, suggesting that *daf-16* regulates the expression of *col-19p::gfp* specifically in the dauer life history (Wirick et al. 2021).

In addition to fluorescent markers, there are several other adult-specific characteristics that are commonly used to characterize larval vs. adult cell fate. We found that *daf-16(0)* PD adults showed penetrant defects in all of these characteristics examined (Figure 1B-C). We first measured the expression of adult alae which are secreted by seam cells upon the larval/adult switch to form a continuous cuticular structure along each lateral side of the adult animal (Sulston and Horvitz 1977; Ambros and Horvitz 1984). *daf-16(0)* mutant PD adults displayed gapped or missing alae, consistent with some or all seam cells failing to adopt adult cell fate (Figure 1B). Next, we observed adherence junctions using an *ajm-1::gfp* reporter. Junctions are present between seam cells in larvae but not in adults since seam cells fuse with each other to form a seam syncytium (Podbilewicz and White 1994). While many seam cells fused, at least one junction was still evident in more than half of *daf-16(0)* PD adults (Figure 1C). As with *col-19p::gfp* expression, we found that these defects were only present in mutants that had developed through dauer; *daf-16(0)* adults that developed continuously did not express defects in alae or seam cell junctions (Figure 1B-C). Taken together, these results suggest that *daf-16* functions specifically in the dauer life history to promote adult seam cell fate.

We next wondered which isoforms of *daf-16* contribute to the regulation of adult cell fate after dauer. There are three major isoforms of *daf-16* (*a, b, and f*) that participate differently in longevity, dauer formation and neuronal development (Chen et al. 2015; Sun et al. 2019). During dauer, we showed that all three isoforms were required to oppose the expression of *col-19p::gfp* (Wirick et al. 2021). In a similar manner, we took advantage of isoform-specific mutants (Chen et al. 2015) to assess the expression of adult alae and *col-19p::gfp* in PD adults. We found that while loss of the individual *daf-16(a)* or *daf-16(f)* isoforms did not result in penetrant defects, the combined loss of these two isoforms did result in penetrant defects, particularly with respect to alae formation (Figure 1D-E). However, the null allele showed stronger defects than the *daf-16(a,f)* mutant, suggesting that the *daf-16(b)* isoform also contributes (Figure 1D-E). Taken together, we conclude that all three major isoforms of *daf-16* contribute to the regulation of adult cell fate after dauer.

In the course of performing the experiments described above, we noticed that *daf-16(0)* mutants required an extra day to recover from dauer, relative to control larvae. This observation is consistent with a previous report (Chen and Riddle 2008). To quantify this phenotype in our hands, we measured the percent of dauer larvae that failed to recover 24 hours after shifting dauer larvae from 24°C to 20°C and observed that the majority of *daf-16(0)* larvae remained in dauer, while control larvae had largely resumed development at this time (Figure 1F). This led

us to ask if the additional time that *daf-16(0)* larvae spent in dauer contributed to the adult cell fate defects. We assessed alae formation in control and *daf-16(0)* populations at 2 and 3 days after shifting dauer larvae from 24°C to 20°C. At 2 days, most control animals and a few *daf-16(0)* animals had reached adulthood. At 3 days, most *daf-16(0)* animals had reached adulthood and some of the control animals that had not reached adulthood at 2 days were now adults. The control PD adults had very few alae defects at either 2 or 3 days, indicating that time in dauer *per se* does not lead to alae defects (Figure S2). However, *daf-16(0)* 2-day post-recovery adults had substantially fewer alae defects than the *daf-16(0)* 3-day post-recovery adults (Figure S2). These results suggest that for *daf-16* mutants, these two phenotypes may be connected.

daf-16 promotes LIN-29 expression and the transcription of the *let-7*-family miRNAs

Since *daf-16(0)* PD phenotypes are similar to reiterative heterochronic mutant phenotypes, we hypothesized that *daf-16* may regulate heterochronic genes to control the developmental timing of seam cells. *lin-29* is the most downstream heterochronic gene responsible for the larval/adult switch and is required for adult cell fate characteristics including the transcriptional activation of *col-19*, expression of adult alae, and seam cell fusion, with each of its two isoforms (*lin-29a* and *lin-29b*) responsible for a different subset of those fates (Ambros and Horvitz 1984; Rougvie and Ambros 1995; Azzi et al. 2020). We first asked if *daf-16* regulates LIN-29 expression after dauer. We assessed the expression pattern of LIN-29 in control and *daf-16(0)* PDL4 larvae using an endogenously tagged allele of *lin-29*, *lin-29::gfp* (Aeschimann et al. 2019), and found that *daf-16(0)* PDL4 larvae expressed LIN-29::GFP in fewer hypodermal nuclei than control PDL4 larvae (Figure 2A). In particular, the majority of *daf-16(0)* PDL4 larvae expressed LIN-29::GFP in an L3-like pattern where expression was primarily in the seam cell nuclei and less in hyp7 (Azzi et al. 2020). This expression pattern is consistent with the reiterative phenotypes in *daf-16(0)* PD adults. Surprisingly, RNAi depletion of *lin-41* and *hbl-1*, the two most direct negative regulators of *lin-29* known, failed to suppress defects in LIN-29::GFP expression and adult alae in *daf-16(0)* PD animals (Figure S3A-B) (Fay et al. 1999; Slack et al. 2000; Abrahante et al. 2003; Lin et al. 2003; Azzi et al. 2020). This lack of suppression may be because *hbl-1* and *lin-41* function redundantly to regulate LIN-29 expression or because RNAi treatment may not have sufficiently depleted *hbl-1* and *lin-41*. Alternatively, *lin-29* may be regulated via a different mechanism in post-dauer animals. Taken together, we found that *daf-16* promotes the expression of LIN-29 in hypodermal cells,

consistent with the role of *daf-16* in promoting adult cell fate after dauer, though the mechanism by which *daf-16* regulates LIN-29 remains unclear.

We next wondered if *daf-16* regulates miRNAs to control the larval/adult switch. Mutations of heterochronic miRNAs result in reiterative phenotypes, similar to those we saw in *daf-16(0)* post-dauer animals (Chalfie et al. 1981; Reinhart et al. 2000; Abbott et al. 2005). To broadly test if *daf-16* regulates miRNAs to control the larval/adult switch, we crossed worms with a null mutation in one of the major miRNA-specific Argonaute proteins, *alg-1(0)*, into our *daf-16(0)* background. *alg-1(0)* mutants display reiterative phenotypes during continuous development but strikingly have little to no defects after dauer, suggesting that the other major somatic miRNA-specific Argonaute protein, ALG-2, is sufficient for the larval/adult switch in the post-dauer context (Karp and Ambros 2012). Though *alg-2* may be sufficient after dauer, we hypothesized that loss of *alg-1* would create a miRNA-sensitized background for our study in post-dauer animals. Indeed, when observing alae in PD adults, we found an enhancement in alae defects in the *daf-16(0); alg-1(0)* double mutant relative to the *daf-16(0)* single mutant (Figure 2B).

let-7-family miRNAs *(mir-48, mir-84, mir-241, let-7)* are attractive candidates to regulate PD adult cell fate downstream of *daf-16.* During continuous development, these miRNAs promote adult cell fate by downregulating *hbl-1* and *lin-41* as their primary targets (Reinhart et al. 2000; Abbott et al. 2005). In the dauer life history, the *let-7* sisters: *mir-48, mir-84,* and *mir-241* function in parallel with the *lin-4* miRNA to promote L3 cell fate (Karp and Ambros 2012). Loss of *mir-48*, *mir-84*, and *mir-241* results in penetrant adult cell fate defects during continuous development, but not in the dauer life history, unless combined with mutations in other miRNAs. In contrast, *let-7* mutants display penetrant adult cell fate defects in both life histories (Reinhart et al. 2000; Hansen et al. 2022). We found that loss of the 3 *let-7* sisters did not enhance the *daf-16(0)* phenotype in PD adults, in contrast to the enhancement observed between *daf-16(0)* and *alg-1(0)* mutants (Figure S4A). This observation suggests that other miRNAs, such as *let-7,* may also regulate PD adult cell fate in this context. To address the possibility that *let-7* may function with the other *let-7*-family miRNAs after dauer, we crossed worms with the temperature sensitive *let-7(n2854)* (hereafter: *let-7(-)*) allele with worms harboring a *mir-241(0)* allele and asked if loss of *mir-241* could enhance adult alae defects in *let-7(-)* mutants. We found a 16% increase in adult alae defects in the double mutant, compared to the *let-7(-)* mutant, though this difference was not statistically significant (Figure S4B).

To more directly test whether *daf-16* regulates the *let-7*-family miRNAs, we next examined whether miRNA levels change when *daf-16* is removed. We used qRT-PCR to quantify the levels of mature *let-7*-family miRNAs in *daf-16(0)* and control PDL4 larvae and found that *mir-84*, *mir-241*, and *let-7* were downregulated in *daf-16(0)* PD larvae (Figure 2C). To test whether this downregulation was mediated transcriptionally, we first observed the expression of a fosmid-based *let-7* transcriptional reporter and found that *let-7* transcription was modestly dampened in the *daf-16(0)* PDL4 larvae, consistent with the modest downregulation of levels of mature *let-7* (Figure 2D). This difference was not observed in PDL3 larvae, but the expression was highly variable at this stage (Figure S5). The expression of the *let-7*-family miRNAs has been reported to be oscillatory during larval stages, which would not be captured by the stable GFP in the *let-7p::gfp* transcriptional reporter (Patel et al. 2022). To more accurately measure the transcriptional control of a *let-7* family miRNA, we obtained an endogenous *mir-241* transcriptional reporter that includes a PEST. We compared the expression of *mir-241p::mScarlet* in *daf-16(0)* and control PD larvae at the PDL3 molt and found a strong downregulation of the reporter in *daf-16(0)* PDL3m larvae compared to control larvae (Figure 2E). Whereas control PD larvae robustly expressed this marker, *daf-16(0)* PD larvae expressed *mir-241p::mScarlet* dimly or not at all (Figure S6). Together, these results suggest that *daf-16* promotes the transcription of the *let-7* family miRNAs after dauer.

We next asked how *daf-16* might regulate the transcription of the *let-7* family miRNAs. During continuous development, NHR-23/ROR directly activates the transcription of all *let-7* family miRNAs (Hayes et al. 2006; Patel et al. 2022). NHR-23 activates the expression of *let-7* and other targets though binding to retinoid orphan receptor elements (RORE) in promoter regions (Kouns et al. 2011; Patel et al. 2022). We hypothesized that *daf-16* may promote the expression of *nhr-23*, which would activate the transcription of the *let-7* family miRNAs after dauer. To test this, we used the auxin-inducible degron system to deplete NHR-23 (Zhang et al. 2015). To avoid the molting defects that occur when NHR-23 is broadly depleted in somatic cells, we used a seam cell-specific driver to express the TIR1 E3 ubiquitin ligase (Ashley et al. 2021; Johnson et al. 2023). Depletion of NHR-23 after dauer in control animals resulted in moderate adult alae defects (Figure 2F). Surprisingly, in contrast to what was observed during continuous development, disruption of all three RORE sites in the *let-7* promoter (hereafter, *let-7(scRORE)*) did not phenocopy depletion of NHR-23, suggesting that *nhr-23* acts through additional targets in this context. When we combined depletion of NHR-23 with loss of *daf-16,* we observed more penetrant alae defects than observed in either of the single mutants, suggesting that *daf-16* and *nhr-23* act in parallel to regulate adult cell fate after dauer (Figure

2G). Similar to what we saw in the wild-type background, *let-7(scRORE)* did not recapitulate the depletion of NHR-23, indicating that *let-7* is not the sole target of NHR-23 (Figure 2G). Taken together, these data suggest that *daf-16* regulates adult cell fate at least partially in parallel to *nhr-23*.

daf-16 promotes the liganded DAF-12 complex

Since *daf-16* appears to act in parallel rather than upstream of *nhr-23,* we next wondered which other genes *daf-16* might regulate to impact levels of *let-7*-family miRNAs. Another known mechanism by which these miRNAs are transcriptionally regulated is by the DAF-12 nuclear hormone receptor. In favorable conditions, the DAF-12 ligand dafachronic acid (DA) is synthesized from exogenous cholesterol consumed by the worm (Figure 3A) (Aguilaniu et al. 2016). The activating DAF-12-DA complex functions to promote continuous development and the expression of the *let-7*-family miRNAs (Antebi et al. 1998; Motola et al. 2006; Bethke et al. 2009; Hammell et al. 2009). In unfavorable conditions, the gene encoding the enzyme that catalyzes the final step in the DA biosynthetic pathway, *daf-9*, is downregulated through the TGFb and insulin/IGF signaling pathways, resulting in low levels of DA (Gerisch and Antebi 2004; Mak and Ruvkun 2004). In the absence of DA, DAF-12 binds its corepressor, DIN-1S, to promote dauer formation and repress the transcription of the *let-7*-family miRNAs (Antebi et al. 1998; Ludewig et al. 2004; Bethke et al. 2009).

To test if *daf-12* regulates seam cell fate after dauer, we first thought to use the AID system to conditionally deplete DAF-12 in somatic tissue; a null allele would not be useful since *daf-12* activity is needed for dauer formation (Antebi et al. 1998; Zhang et al. 2015). After crossing the *daf-12(aid)* and *daf-7(e1372)* alleles together, we noticed an increased number of dauer larvae in populations at 20°C. To quantify this enhanced Daf-c phenotype, we grew synchronized populations of *daf-7; daf-12(aid)* and control *daf-7* embryos at 20°C and found that only ~14% of the *daf-12(aid)* animals bypassed dauer compared to ~48% of control larvae (Figure S7). This enhanced Daf-c phenotype is reminiscent of *daf-9(0)* mutants that fail to produce DA, or *daf-12(rh273)* mutants that bind DA poorly, thus shifting the DAF-12 complex to its repressive form (Antebi et al. 1998; Gerisch et al. 2001). In addition to dauer defects, *daf-12(rh273)* mutants also display reiterative heterochronic defects (Antebi et al. 1998). We reasoned that if this *daf-12(aid)* allele has enhanced Daf-c phenotypes due to an increased proportion of DAF-12 in its unliganded, repressive form, then we would observe defects in adult alae in these mutants due to reduced expression of *let-7*-family miRNAs. Since *daf-12* is required for dauer formation and dauer exit (Antebi et al. 1998; Zhang and Sternberg 2022), we

induced dauer formation and then recovery before addition of auxin, moving larvae to plates containing auxin only after recovery at 20°C for 12 hours. These animals remained on auxin plates until they reached adulthood. In agreement with our hypothesis, we found that *daf-12(aid)* PD adults displayed penetrant alae defects in the absence of auxin. These defects were caused by the *daf-12(aid)* allele because they were suppressed upon somatic depletion of DAF-12 (Figure 3B).

We next hypothesized that *daf-16(0)* PD animals may have elevated activity of the repressive DAF-12 complex, leading to reduced levels of *let-7*-family miRNAs. To test this hypothesis, we first treated *daf-16(0)* dauer larvae with 100nM Δ7-DA to promote the activating DAF-12 complex and assessed alae morphology in PD adults. Treatment with Δ7-DA almost completely suppressed alae defects in *daf-16(0)* PD adults, while *daf-16(0)* animals treated with ethanol as a carrier control retained penetrant alae defects (Figure 3C). We also tested intermediates in the DA biosynthetic pathway to determine if they may also suppress alae defects in *daf-16(0)* PD adults (Figure 3A). All intermediates tested suppressed alae defects in *daf-16(0)* PD adults to some degree, except for the starting sterol, cholesterol, which is already in abundance in the NGM media (Figure 3C). This suppression of adult alae defects in *daf-16(0)* PD adults by Δ7-DA treatment coincided with the rescue of *let-7p::gfp* and *mir-241p::mScarlet* expression in PDL4 and PDL3m larvae, respectively (Figure 3D-E and Figure S8).

We also assessed adult alae in the contexts where *daf-16(0)* and *nhr-23(aid)* or *alg-1(0)* alleles synergized. We found that Δ7-DA treatment suppressed alae defects in *nhr-23(aid) daf-16(0)* PD adults back to the levels observed in *nhr-23(aid)* adults, consistent with *daf-16* acting via DA and DAF-12, and *nhr-23* acting via an independent pathway (Figure S9A). The addition of Δ7-DA to *daf-16(0); alg-1(0)* animals only partially suppressed the defects in adult alae (Figure S9B). Since ALG-1 is involved in both biosynthesis and activity of miRNAs, restoring the transcription of the *let-7*-family miRNAs may not be sufficient to restore full activity. Alternatively, other miRNAs may contribute to the phenotype.

We next asked if the activity of the repressive DAF-12 complex could contribute to the dauer recovery defects observed in *daf-16(0)* mutants (Figure 1F). As previously mentioned, liganded form of DAF-12 is required for dauer exit (Zhang and Sternberg 2022). Similar to the assessment of adult alae, we treated *daf-16(0)* dauer larvae with either an ethanol carrier control, Δ7-DA, cholesterol, or intermediates in the DA biosynthetic pathway (Figure 3A). We found that the addition of Δ7-DA or any of the intermediates suppressed the dauer recovery defects in *daf-16(0)* animals, while cholesterol did not (Figure 3F). To ask if the suppression of

dauer recovery defects by Δ7-DA treatment is specific to instances where the activity of the repressive DAF-12 complex is increased, we treated control dauer larvae with ethanol or Δ7-DA and found no significant increase in dauer recovery (Figure 3G). Taken together, these results suggest that *daf-16* coordinates the exit from dauer and the resumption of seam cell development by promoting the activity of the liganded DAF-12 complex.

daf-16 **functions before dauer to promote adult cell fate and cholesterol retention after dauer**

We next asked how *daf-16* might promote the liganded DAF-12 complex. A simple hypothesis is that *daf-16* might promote the expression of an enzyme within the DA biosynthetic pathway. However, mRNA-seq data comparing *daf-16(0)* and control dauer larvae showed that no known enzymes in this pathway are downregulated in *daf-16(0)* dauer larvae (Figure 3A) (Wirick et al. 2021). Furthermore, as described above, multiple intermediates in the DA biosynthetic pathway suppressed PD *daf-16(0)* defects (Figure 3C, F). These results suggest that DA may be limiting in *daf-16(0)* PD larvae and that the mechanism by which *daf-16* promotes DA production lies somewhere upstream of the conversion of cholesterol to 7-dehydrocholesterol (Figure 3A). Recently, it was reported that cholesterol sequestered in the intestinal lumen of dauer larvae is required to synthesize DA upon dauer recovery (Schmeisser et al. 2024). Little is known about this process, but two key genes encoding proteins that appear to bind cholesterol in the gut lumen and mediate its sequestration are *scl-12* and *scl-13* (Schmeisser et al. 2024). To ask if these cholesterol-sequestering genes are misregulated in *daf-16(0)* dauer larvae, we again examined our mRNA-Sequencing data from *daf-16(0)* and control dauer larvae and found that both *scl-12* and *scl-13* are strongly downregulated in *daf-16(0)* dauer larvae (Figure 4A) (Wirick et al. 2021). We then conducted ChIP-Sequencing on populations of dauer larvae with endogenous *daf-16* tagged with 3xflag and on control untagged wild-type (N2). We found that DAF-16 was enriched in two peaks in the shared promoter region between *scl-12* and *scl-13,* suggesting that DAF-16 may directly bind the promoters of these genes to activate their expression (Figure 4B). To ask if the downregulation of *scl-12* and *scl-13* correlated with a lack of sequestered cholesterol, we administered TopFluor™ Cholesterol (Avanti Research), which reports cholesterol localization, to larvae during dauer formation and found that surprisingly, *daf-16(0)* dauer larvae appeared to sequester a greater amount of cholesterol in the gut lumen than control dauer larvae (Figure 4C). We note that *daf-16(0)* dauer larvae display a larger intestinal lumen than controls, so the apparent increased levels of TopFluor Cholesterol may be a result of the intestinal lumen having a larger volume. We also

observed the expression of endogenously tagged *scl-12* allele, *scl-12(mScarlet)* (Schmeisser et al. 2024), in the strains assessed for TopFluor Cholesterol and in agreement with our mRNA-Sequencing data, SCL-12 expression was not detectable in *daf-16(0)* dauer larvae (Figure 4C).

The presence of apparently sequestered TopFluor Cholesterol in *daf-16(0)* dauer larvae led us to wonder what happens to cholesterol when the larvae exited dauer. Upon dauer recovery, cholesterol bound to SCL-12 is mobilized from the gut lumen and released to become available for DA biosynthesis (Schmeisser et al. 2024). We asked if cholesterol was properly trafficked as *daf-16(0)* dauer larvae were recovering. To drive dauer recovery, we treated control and *daf-16(0)* dauer larvae, that were previously fed TopFluor Cholesterol, with 100nM Δ7-DA. After 7 hours of development on plates containing Δ7-DA, we noticed that a large fraction of *daf-16(0)* larvae no longer contained detectable TopFluor Cholesterol signal in the gut lumen and instead accumulated in what appeared to be an expanded cuticle region at the posterior end of the larvae (Figure 4D-E). In contrast, TopFluor Cholesterol was still visible in the intestinal lumen of control larvae at this same time point (Figure 4D-E). We also observed SCL-12::mScarlet expression at this time point, which remained undetectable in *daf-16(0)* larvae, suggesting that the loss of TopFluor Cholesterol signal was unlikely to be mediated by SCL-12 (Figure 4D). These findings suggest that *daf-16(0)* larvae fail to retain cholesterol in the gut lumen upon dauer recovery, resulting in the defecation and loss of cholesterol that was stored during dauer.

daf-16 functions cell non-autonomously and prior to dauer formation to regulate adult cell fate after dauer

We next asked when *daf-16* acts to promote adult cell fate after dauer. SCL-12::mScarlet expression begins prior to dauer entry as cholesterol sequestration initiates (Schmeisser et al. 2024). If *daf-16* promotes the retention of cholesterol through genes that sequester cholesterol during dauer, then we reasoned that *daf-16* would be required before dauer to promote adult cell fate in PD adults. We conditionally depleted DAF-16 in somatic tissue using the AID system either throughout dauer development, before dauer formation, or after dauer formation had occurred and assessed alae formation in PD adults (Figure 5A). We found that depletion of DAF-16 before dauer resulted in alae defects, regardless of whether DAF-16 was depleted after dauer (Figure 5B). To narrow down the window when *daf-16* is required, we depleted DAF-16 for different amounts of time before dauer formation as well as during dauer formation. Specifically, we began auxin treatment at 36, 42, or 48 hours after embryo isolation. These timepoints correspond to approximately 12, 6, or 0 hours before dauer formation, respectively. At 50 hours after embryo isolation, larvae were shifted to 20°C to induce dauer recovery. Alae

were then assessed in worms had developed into PD adults (Figure 5A). We found that depletion of DAF-16 during dauer or 6 hours before dauer formation did not result in PD alae defects, while depletion 12 hours before dauer formation did (Figure 5C). We also assessed dauer recovery for these same conditions and found similar results, where only depletion of DAF-16 12 hours prior to dauer formation produced a dauer recovery phenotype (Figure 5D). Taken together, these results suggest that DAF-16 is required before dauer to promote adult seam cell fate in PD adults.

We next wondered which tissues DAF-16 expression is required in for dauer recovery and PD adult cell fate. If *daf-16* regulates these processes through cholesterol retention upon dauer recovery, then we hypothesized that *daf-16* would be required in intestinal tissue to promote dauer recovery and adult cell fate after dauer. We again utilized the AID system to deplete DAF-16 throughout dauer development but expressed TIR1 under various tissue-specific promoters (Figure 5E). While none of the tissue-specific depletions recapitulated the dauer recovery phenotypes seen with ubiquitous somatic depletion (Figure S11), we found that depletion of DAF-16 in the intestine resulted in a moderate, yet statistically significant, alae defect (Figure 5F). In contrast, depletion DAF-16 in other tissues, including the hypodermis, resulted in few if any alae defects (Figure 5F). Similar to our observations using the *daf-16* null allele, we found that depletion of DAF-16(aid) only resulted in alae defects in animals that were delayed in dauer recovery, consistent with the hypothesis that dauer recovery and adult cell fate are connected in this context (Figure S2 and Figure S10).

Finally, we wondered if the focus for *daf-16* in opposing *col-19p::gfp* during dauer was also the intestine or whether *daf-16* might act cell-autonomously in this context. We found that depletion of DAF-16 in the hypodermis resulted in a modest increase in dauer larvae expressing *col-19p::gfp* while depletion of DAF-16 in other tissues, including the intestine, did not (Figure S12), suggesting that *daf-16* blocks *col-19p::gfp* cell autonomously during dauer.

In sum, we propose that *daf-16* acts before dauer formation to promote the retention of cholesterol in the gut lumen upon dauer recovery; cholesterol is synthesized into DA which then binds to DAF-12. The activating DAF-12-DA complex then promotes dauer recovery and then in PD larvae promotes the transcription of the *let-7* family miRNAs, leading to the transition from larval to adult seam cell fate.

Discussion

The regulation of stage-specific seam cell fate and the transition from larval to adult cell fate is coordinated by heterochronic genes (Ambros and Horvitz 1984). The DAF-12-DA complex transcriptionally actives the expression of the *let-7*-family miRNAs and promotes continuous development (Antebi et al. 1998; Bethke et al. 2009; Hammell et al. 2009). The repressive ligand-free DAF-12 complex drives dauer formation and pauses seam cell development by repressing the expression of the *let-7* family miRNAs (Antebi et al. 2000; Ludewig et al. 2004; Bethke et al. 2009; Hammell et al. 2009). We have previously shown that *daf-16* also functions to adult cell fate during dauer (Wirick et al. 2021). If environmental conditions improve, *daf-16* and *daf-12* both function to promote dauer exit (Chen and Riddle 2008; Zhang and Sternberg 2022). In contexts where DAF-12 persists in its repressive form after dauer, such as *daf-12(rh273)* mutants that poorly bind DA, adults express defects in adult cell fate, suggesting that the activating DAF-12/DA complex may coordinate dauer recovery and the resumption of seam cell development (Antebi et al. 1998). Here, we find that *daf-16* promotes the activating DAF-12 complex through retention of cholesterol during the dauer recovery process.

We show that defects in dauer recovery correlated with defects in adult cell fate, specifically adult alae, in *daf-16(0)* mutants (Figure 1A-C). We found that the small fraction of *daf-16(0)* larvae that were not delayed in recovery from dauer displayed very few defects in adult alae, in contrast to the majority of *daf-16(0)* larvae that took longer to recover from dauer arrest that displayed penetrant alae defect (Figure 1F, Figure S2). We propose that this difference in *daf-16(0)* PD adults that recovered at different rates is directly correlated with the levels of cholesterol retained upon dauer recovery. In *daf-16(0)* recovering dauer larvae, we found that most, but not all, animals lacked detectable levels of TopFluor cholesterol in the gut lumen, indicating improper retention of cholesterol (Figure 4C). We speculate that the *daf-16(0)* larvae that retained TopFluor cholesterol during dauer recovery may produce enough DA to allow the activating DAF-12 complex to promote dauer recovery without delay and to allow the expression of adult cell fate in PD adults. *scl-12* and *scl-13* have been previously shown to be required for the sequestration of cholesterol in the gut lumen of dauer larvae (Schmeisser et al. 2024). Interestingly, though mRNA and protein levels of *scl-12* and *scl-13* were robustly downregulated in *daf-16(0)* dauer larvae, TopFluor cholesterol signal was still present in the gut lumen of *daf-16(0)* dauer larvae prior to recovery (Figure 4A, C). The residual expression of *scl-12* and *scl-13* in *daf-16(0)* dauer larvae could be sufficient to sequester cholesterol during dauer,

but not to retain cholesterol during dauer recovery. Additionally, there may be other compensatory mechanisms that can sequester, but not retain, cholesterol, such as the 4 of the 25 other SCL genes encoded in the genome of *C. elegans* that are misregulated in *daf-16(0)* dauer larvae (Wirick et al. 2021).

Our model suggests that *daf-16* promotes the retention of cholesterol during dauer recovery. We propose that *daf-16* acts at this point in the DA biosynthetic pathway for the following reasons. First, there is no evidence for a defect in cholesterol uptake in *daf-16(0)* animals. *C. elegans* cannot synthesize cholesterol *de novo* and therefore relies on uptake of exogenous cholesterol (Chitwood 1997). Consistent with proper uptake of cholesterol, TopFluor cholesterol was present in the gut lumen of *daf-16(0)* dauer larvae (Figure 4C). Additionally, the cholesterol transporting genes, *ncr-1* and *ncr-2*, are not misregulated in *daf-16(0)* dauer larvae, which suggests that cholesterol can be transported during dauer (Sym et al. 2000; Wirick et al. 2021). The defects in dauer recovery and adult cell fate were also suppressed to some degree when all of the intermediates in the DA biosynthesis pathway were administered to *daf-16(0)* dauer larvae (Figure 3C, D), suggesting that the enzymatic steps that convert cholesterol to DA are not compromised in *daf-16(0)* PD animals. Taken together, these data indicate that *daf-16* regulates the bioavailability of cholesterol at some point after cholesterol is taken up by the worm and before cholesterol is enzymatically converted in the DA biosynthetic pathway. The maintenance of cholesterol stores in the gut lumen fits in this window.

We have previously shown that *daf-16(0)* mutants display a different phenotype during dauer, where adult-enriched collagens and *col-19p::gfp* are misexpressed. One explanation for the lack of adult cell fate characteristics in *daf-16(0)* PD adults could be that these defects are a consequence of the precocious adult cell fate expressed during dauer. However, we were able to separate these phenotypes in several ways. First, we showed that after dauer, defects in adult alae were suppressed when *daf-16(0)* dauer larvae, which presumably expressed *col-19p::gfp*, were treated with Δ7-DA (Figure 4C). Additionally, the tissue-specific depletion of DAF-16 experiments provide evidence that DAF-16 functions in different tissues to regulate seam cell fate during and after dauer. Depletion of DAF-16 in the hypodermis induced a modest increase in the expression of *col-19p::gfp* during dauer, but did not affect the expression of adult alae after dauer (Figure 5F and Figure S12). In contrast, dauer larvae with DAF-16 depleted in intestinal tissue did not express *col-19p::gfp*, while this depletion resulted in adult alae defect after dauer (Figure 5F and Figure S12). In both cases, the ectopic expression of *col-19p::gfp* and the defects in adult alae from hypodermal and intestinal depletions of DAF-16, respectively,

never completely phenocopied the defects observed in broad somatic depletion of DAF-16. This may be due to reduced expression of the tissue-specific drivers, *dpy-7* and *ges-1,* during dauer, compared to non-dauer stages, as shown on Wormbase (WS296) (Gerstein et al. 2010) . Alternatively, *daf-16* activity in multiple tissues may contribute to its function. In sum, our findings provide evidence that the roles for *daf-16* in opposing *col-19p::gfp* during dauer and in promoting adult cell fate after dauer are distinct.

Lastly, we have identified a novel connection between dauer formation *(daf)* genes and the heterochronic pathway. As mentioned, *daf-12* is required for the dauer formation decision and for the temporal patterning of seam cells (Antebi et al. 1998; Bethke et al. 2009; Hammell et al. 2009). Similarly, *daf-16* promotes dauer formation and acts during dauer through *lin-41* to oppose *col-19p::gfp* expression (Ogg and Ruvkun 1998; Wirick et al. 2021). Furthermore, other heterochronic genes, including *lin-42, hbl-1*, and *lin-41*, have also been implicated in the decision to enter dauer (Tennessen et al. 2010; Karp and Ambros 2011; Cale and Karp 2020). After dauer, we show that *daf-16* indirectly regulates the transcription of the *let-7*-family miRNAs through DA and DAF-12. Some heterochronic mutants, including those lacking *mir-48, mir-84*, and *mir-241*, display defects in adult cell fate during continuous development, but not after dauer, suggesting a difference in how seam cells are regulated between these life histories (Liu and Ambros 1991; Karp and Ambros 2012). The connection between *daf-16* and *daf-12* in the regulation of seam cell fate after dauer that we show provides new insight into the mechanisms that modulate the heterochronic pathway in different life histories.

Methods

Strains and maintenance

All *C. elegans* strains were grown at 15°C or 20°C on standard Nematode Growth Medium (NGM) plates and seeded with *E. coli* OP50 (Brenner 1974). Strains used in this study can be found in Table S1.

Synchronizing continuously developed worms

For Figures 1B-C, gravid adults were allowed to lay embryos at 25°C for 6 hours. Adults were removed from the plates and embryos were allowed to develop at 25°C for 24 hours, then were shifted to 15°C until they reached adulthood.

Dauer induction

All strains that developed through the dauer life history in this study contained the *daf-7(e1372)* temperature sensitive allele which forms constitutive dauer larvae at 24-25°C (Vowels and Thomas 1992; Karp 2018). With exceptions noted below, populations of embryos were obtained from plates with gravid adults that were treated with two 2-minute incubations of 1M NaOH, 10% sodium hypochlorite, then washed twice with dH_2O. Embryos were plated onto NGM plates seeded with OP50 and incubated at 24°C for approximately 50 hours to allow larvae to enter dauer.

For Figures 1A-C, 1E-F, and S1, gravid adults were allowed to lay embryos on NGM plates seeded with OP50 for 2-8 hours at 24-25°C. Adults were removed from the plates and embryos were incubated at 24-25°C for 48-52 hours to allow dauer larvae to form.

For Figure 4B, embryos were obtained by sodium hypochlorite treatment, suspended in M9 buffer, and incubated for 24 hours with aeration at room temperature. Starved L1d hatchlings were plated on NGM plates seeded with E. coli strain HB101. 15000 hatchlings were plated on 15 cm NGM plates seeded with 10X concentrated HB101 at 25°C on Day 1. The animals were re-fed on Day 3 and starved worms were subject to SDS isolation on Day 5. Starved worms were incubated with 1% SDS in water for 30 min with aeration. Worms were washed with water and plated on 15 cm NGM plates to allow viable worms to move out. The dead worms were removed from the plate and rest were collected for ChIP-seq.

Post-dauer populations

Once populations of dauer larvae were obtained, they were manually picked to a new NGM plate seeded with OP50 and shifted to 20°C, unless otherwise specified. For Figures 1A-C, 1E-F, S4B, dauer larvae were recovered at 15°C.

Generally, *daf-16(wt)* PD adult were assessed 2 days after shifting dauer larvae from 24°C to 15-20°C. *daf-16(-)* mutants required an additional day. In experiments where PD adults were assessed on both 2 and 3 days after dauer recovery, adults were observed on the second day. All other adults were removed from the plates and the residual PD larvae were allowed to develop into adulthood for one more day.

Compound microscopy

Animals were mounted onto glass slides with 2% agarose pads and immobilized with 0.1M levamisole. A Zeiss AxioImager D2 compound microscope with HPC 200 C or X-cite Xylis II fluorescent optics was used to image animals. DIC and fluorescence images were captured with

a AxioCam MRm Rev 3 or Axiocam 807 mono camera and ZEN 3.2-10 software. GFP images were captured with a high efficiency GFP shift free filter and mScarlet images were captured with a Zeiss 63HE filter.

Phenotypic analysis

Adult alae in adults were observed with DIC optics along the lateral cuticle of the worm, between the rectum and pharynx. An adult was classified to have “gapped” alae if alae were present above some but not all seam cells, while worms lacking any detectable alae were classified as “missing”.

To determine the expression intensity of *col-19p::gfp* in adults (Figure 1D-E), control animals were imaged first, to give the experimenter a baseline for *col-19p::gfp* expression. *daf-16(0)* mutants were then assessed using the same fluorescence settings and assigned “dim” if the expression of *col-19p::gfp* was dimmer than was commonly found in control adults, and “off” if *col-19p::gfp* expression was not detectible. For *col-19p::gfp* expression in Figure 1A, an animal was determined to express *col-19p::gfp* if any hypodermal nuclei had detectable expression.

The *ajm-1::gfp* reporter was captured in GFP images. Worms were classified with having junctions when the expression of *ajm-1::gfp* was detectable between seam cells. Some animals had regions of *ajm-1::gfp* that did not connect between adjacent seam cells, which we noted as “evidence of divisions” (Figure 1C) (Podbilewicz and White 1994).

To determine the penetrance of *col-38p::yfp*, L2d larvae were assessed 28hr after embryo laying, L2dm larvae were assessed 38 hours after embryo laying, and dauer larvae were assessed 48hr after embryo laying. For post-dauer stages, dauer larvae were picked to fresh plates to recover at 20°C. PDL3 and PDL4 larvae were assessed for *col-38p::yfp* expression 24-72hr after placement at 20°C. To verify larvae were not yet in dauer (L2d) or had recovered from dauer (PDL3), fluorescent beads were used to demonstrate that larvae were pumping and consuming food (Nika et al. 2016). The extension of gonad arms was used to distinguish between PDL3 and PDL4 larvae. Adults were determined by the presence of embryos.

Fluorescence of *let-7p::gfp* was measured using ImageJ (Version 1.54f) software. Images of an entire larva were captured with DIC and GFP channels on a 10X (Figure 2E) or 20X (Figure 3D) objective. The entire body of a larva from a DIC image was selected as the region of interest (ROI) using the freehand selection tool. That ROI was then measured on the GFP image to give the mean fluorescence intensity of GFP signal for a given worm.

To assess the penetrance of *col-19p::gfp* in dauer larvae, GFP images were captured in the posterior hypodermis of dauer larvae. Dauer larvae were considered to have “bright” *col-19p::gfp* expression if expression in <2 hypodermal nuclei was easily distinguishable from the autofluorescence in the worm body. “Dim” *col-19p::gfp* was determined if expression in <2 hypodermal nuclei was difficult to distinguish from the autofluorescence. Penetrance of *col-19p::gfp* expression was determined by number of larvae expressing *col-19p::gfp* in hypodermal nuclei out of the total number scored.

Dauer larvae and recovering dauer larvae were assessed for TopFluor™ Cholesterol (Avanti Research, CAS: 878557-19-8) sequestration and SCL-12::mScarlet expression in the gut lumen. Recovering dauer larvae were also assessed for TopFluor Cholesterol outside of the worm body. The expression of TopFluor Cholesterol in the gut lumen was assessed by examining the portion of the intestine directly posterior to the pharynx.

PDL4 collection for Taqman qPCR

Populations of PDL4 larvae were obtained as described above. PDL4 larvae were picked into 100µL of dH_2O in tubes, then 1mL TRI-Reagent (Ambion) was added. Samples were incubated at room temperature for 10 minutes before flash freezing. Samples were stored at -80°C.

RNA Isolation

Total RNA isolation was conducted using TRI-Reagent (Ambion) standard protocol with the following modifications: to improve extraction efficiency pelleted *C. elegans* in TRI-Reagent were subjected to three freeze/thaw/vortex cycles prior to BCP addition, isopropanol precipitation was conducted in the presence of glycogen for 2 hours at -80°C, RNA was pelleted by centrifugation at 4°C for 30 minutes at 20,000 x g; the pellet was washed three times in 70% ethanol and resuspended in water. Thermo Scientific Nanodrop2000 was used to determine the concentration and quality of the RNA prior to TaqMan synthesis.

Taqman qPCR analysis

miRNA levels were quantified with a CFX96 Real-Time System (BioRad) using TaqMan assays and probes (Applied Biosystems hsa-let-7a (assay# 000377), cel-miR-48 (assay# 000208), cel-miR-84 (assay# 463262_mat), cel-miR-241(assay# 000249), and U18 (assay# 001764) according to the vendor protocol with modifications as described in (Billi et al. 2012). Relative RNA levels were calculated based on the ΔΔ2Ct method (Nolan et al. 2006) using U18 for

normalization. Results presented are the average of independent calculations from biological duplicates.

Dauer recovery assessment

Populations of dauer larvae were obtained as stated above. Approximately 30-50 dauer larvae were picked to 30mm NMG plates seeded with OP50 and incubated at 20°C for 24 hours. Dauer larvae were distinguished from recovering dauer larvae by radial constriction and pharyngeal pumping. The number of both dauer and non-dauer larvae present on the NGM were counted to give a percentage of larvae remaining in dauer. Larvae that crawled up the side of the petri dish were disregarded.

Conditional depletion of proteins

Stains containing the *nhr-23(xk40)* AID allele were treated with a final concentration of 1mM 3-Indoleacetic Acid (IAA) (Sigma-Aldrich, CAS: 87-51-4) in ethanol dissolved in the molten NGM media. An equal volume of ethanol was added to the media as a carrier control for the IAA treatment. Dauer larvae were picked to 1mM IAA or carrier control plates and recovered at 20°C

Strains containing the *daf-16(ot975)* or *daf-12(ot874)* were treated with a final concentration of 4mM Naphthaleneacetic Acid (KNAA) (PhytoTech Labs, CAS: 15165-79-4) in dH_2O dissolved in NGM media. To correct for the volume of KNAA solution added to the molton NGM, the volume of KNAA to be added was removed from the total volume of water in the NGM media prior to adding the NGM ingredients.

For FigureS 5B, F, Figures S10-12, embryos were obtained by sodium hypochlorite treatment and put onto 4mM KNAA plates or NGM plates seeded with 10X concentrated OP50 and grown at 24°C to induce dauer formation. Dauer larvae were picked to new 4mM KNAA plates or NGM plates seeded with 10X concentrated OP50 and recovered from dauer at 20°C.

For Figures 5C-D, embryos were obtained by sodium hypochlorite treatment (see above) and put onto NGM plates seeded with OP50 and incubated at 24°C. At 36, 42 and 48 hours of incubation at 24°C on NGM, larvae were washed off of the plates with 1M M9 buffer, centrifuged, washed with M9 buffer, distributed to 4mM KNAA plates seeded with 10X concentrated OP50, and incubated at 24°C. Once 50 hours of total incubation at 24°C elapsed, dauer larvae were picked to new 4mM KNAA plates seeded with 10X concentrated OP50 and recovered from dauer at 20°C. Dauer recovery was assessed in a similar fashion as stated above, but on NGM plates with/without KNAA present.

For Figure 3B, dauer larvae were obtained were obtained by sodium hypochlorite treatment added to NGM plates seeded with OP50 and incubated at 24°C.. Dauer larvae were recovered on NGM plates seeded with OP50 at 20°C for 12 hours before being transferred to NGM or 4mM KNAA plates seeded with 10X concentrated OP50. Larvae were then were again incubated at 20°C for an additional 1.5 days before assessing adults.

Daf-c assessment of *daf-12(ot874)*

Synchronized populations of embryos were obtained by sodium hypochlorite treatment and placed onto NGM plates seeded with OP50. Plates with embryos were incubated at 20°C for 3 days, then the number of dauer and non-dauer animals were counted. Dauer larvae were distinguished from non-dauer animals by radial constriction and pharyngeal pumping.

Exogenous sterol treatments

Cholesterol (Sigma Aldrich, CAS: 57-88-5), 7-Dehydrocholesterol (7DHC) (Cayman Chemical, CAS: 434-16-2), Lathosterol (Cayman Chemical, CAS: 80-99-9), and Cholestenone (Cayman Chemical, CAS: 601-57-0) were suspended in pure ethanol to a concentration of 33.3mM. (25S)-Δ^7-Dafachonic acid (DA) (Cayman Chemical, CAS: 949004-12-0) was suspended in pure ethanol to a concentration of 100μM. To test the effect of these sterol molecules, dauer larvae were picked to NGM plates seeded with 10X concentrated OP50 with a single sterol/ethanol solution to a final concentration of 33.3μM for cholesterol, 7DCH, Lathosterol, and Cholestenone, or 100nM for Δ7-DA, based on the volume of the NGM plate. Dauer larvae were then recovered at 20°C.

To determine the best concentration concentration of Δ7-DA to use in this study, we treated *daf-16(0)* dauer larvae with serial dilutions of Δ7-DA. We found that 100nM promotes most *daf-16(0)* dauer larvae to exit dauer (Figure S13).

TopFluor™ Cholesterol treatment

TopFluor Cholesterol was dissolved in pure ethanol to a concentration of 2.5mg/mL. NGM plates without cholesterol added were seeded with 10X concentrated OP50 and TopFluor Cholesterol (final concentration of TopFluor Cholesterol:media, 1:1000). Synchronized populations of embryos were obtained by sodium hypochlorite treatment (see above) and placed onto TopFluor Cholesterol plates. To drive dauer recovery, dauer larvae were recovered on NGM plates containing 100nM Δ7-DA seeded with 10X concentrated OP50.

Chromatin immunoprecipitation for ChIP-Seq

Animals starved at 25°C were collected as a ~500 µL packed pellet in M9. The animals were nutated for 30 min at room temperature in 12mL of 2.6% (v/v) formaldehyde in autoclaved DI water for live crosslinking. To quench the reaction, 600 µL of 2.5 M glycine was added and the worms incubated on the nutatorfor another 5 min. The samples were then washed three times in water and flash- frozen in liquid nitrogen. Frozen pellets were ground twice, for 1 min each, in a Retsch MM400 CryoMill at 30 Hz in liquid nitrogen-chilled stainless steel cryomill chambers, producing a frozen powder of partially lysed worms. The powder was resuspended and further lysed in 2 mL of RIPA buffer (1x PBS, 1% (v/v) NP40, 0.5% sodium deoxycholate, and 0.1% SDS), supplemented with the HALT Protease and Phosphatase Inhibitor Cocktail (ThermoFisher Scientific), for 10 min at 4°C. To shear the chromatin, samples were sonicated in a Bioruptor Pico (Diagenode) for 3 min (30 s ON/30 s OFF cycles), three times, at 4°C. A 20 µL aliquot of the sample was treated with Proteinase K for 10 min and then subjected to phenol chloroform extraction, as described below. The concentration of the aliquot was determined using a Qubit Fluorometer 3.0 (Invitrogen). Based on the initial concentration of the aliquot, the chromatin sample was diluted to 20– 30 ng/µL. To check the extent of shearing, the same aliquot was run on an agarose gel. The sample was processed and analyzed further, provided that the DNA smear centered around 200 bp. Of the total amount of chromatin that remained, 10% was used as the input sample (stored at 4°C) and 90% was subject to immunoprecipitation. Every 10 µg of chromatin was incubated with 2 µg of mouse M2 anti-FLAG monoclonal antibodies (Sigma-Aldrich) overnight at 4°C on a nutator. Next, samples were incubated with 1.5 mg of affinity-purified sheep anti-mouse IgG antibodies covalently attached to superparamagnetic Dynabeads M-280 (Invitrogen) for 2 hours at 4°C. Thereafter, complexes bound to the beads were separated three times from the supernatant and washed in 800 µL LiCl buffer(100 mM Tris-HCL pH 7.5, 500 mM LiCl, 1% (v/v) NP40, and 1% sodium deoxycholate). The resulting immunoprecipitates were de-crosslinked by incubation with 80 µg of Proteinase K in 400 µL of worm lysis buffer (100 mM Tris-HCL pH 7.5, 100 mM NaCl, 50 mM EDTA, and 1% SDS) at 65°C for 4 hours; the input samples also underwent the same treatment in parallel. Residual proteins were removed from both IP and input samples by phenol -chloroform extraction. Briefly, 400 µL of phenol-chloroform-isoamyl alcohol pH 8.0 (Sigma-Aldrich) was added to each sample. The sample was vortexed vigorously and centrifuged at 15,000 x g for 5 min at 4°C. The top layer was transferred to a new tube and DNA was precipitated by incubating with 1 mL of 0.3 M ammonium acetate (Sigma- Aldrich) in ethanol for 1 hour at -30°C. The resulting DNA pellet was washed twice in 100% ethanol and re-suspended in Tris-EDTA, pH 8.0.

Analysis of ChIP-seq data

Demultiplexed raw ChIP-seq data from runs on 2 lanes were concatenated to form one file in FASTQ format. Trim0.5.0 (http://www.bioinformatics.babraham.ac.uk/projects/trim_galore/) was used to trim adaptors and filter for sequencing quality score >Q25. Alignment to the *C. elegans* reference genome WBcel235 was done using Bowtie2 with default parameters. The MarkDuplicates tool in Picard 2.22.1 (http://broadinstitute.github.io/picard/) was used to remove PCR duplicates. MACS 3 callspeak (p value 0.05) tool was used to annotate DAF-16 binding peaks. Samtools was used to generate bigwig files for each replicate for each genotype. The bigwig files were viewed in IGV genome browser. Peaks were assigned to genes within 4kb of the TSS using custom Python scripts.

RNAi

RNAi plates consisted of NGM media containing 50µg/mL Carbenicillin and 200µg/mL IPTG seeded with 250µL of a concentrated overnight culture of RNAi bacteria. Synchronized populations of embryos were obtained by sodium hypochlorite treatment (see above) and placed onto seeded RNAi plates.

RNAi	Source
hbl-1	Source Bioscience (Kamath and Ahringer 2003)
lin-41	Source Bioscience (Kamath and Ahringer 2003)
EV	(Timmons and Fire 1998)

Reproducibility, graphs, and statistical analysis

All data presented were collected from at least two independent experiments performed on different days. Graphs were generated with GraphPad Prism (Version 10.4.1). All statistical analyses were conducted on GraphPad Prism (Version 10.4.1) with the exception of Fisher's Exact Tests which were conducted on VassarStats (vassarstats.net). Statistical analyses that provided a p-value <0.05 were deemed significant. Asterisks denoting significance were used as follows: *p<0.05, **p<0.01, and ***p<0.001. Statistical tests used for each experiment can be found in the respective figure legend.

Acknowledgements

We thank Luisa Cochella (Johns Hopkins University) and Oliver Hobert (Columbia University) for sharing unpublished reagents. We thank Iva Greenwald (Columbia University) and Karp lab members for useful discussions. Some strains were provided by the CGC, which is funded by

NIH Office of Research Infrastructure Programs (P40 OD010440). We thank WormBase. This work was supported by NSF CAREER 1352283 (to XK) and NIH R15GM150082 (to XK).

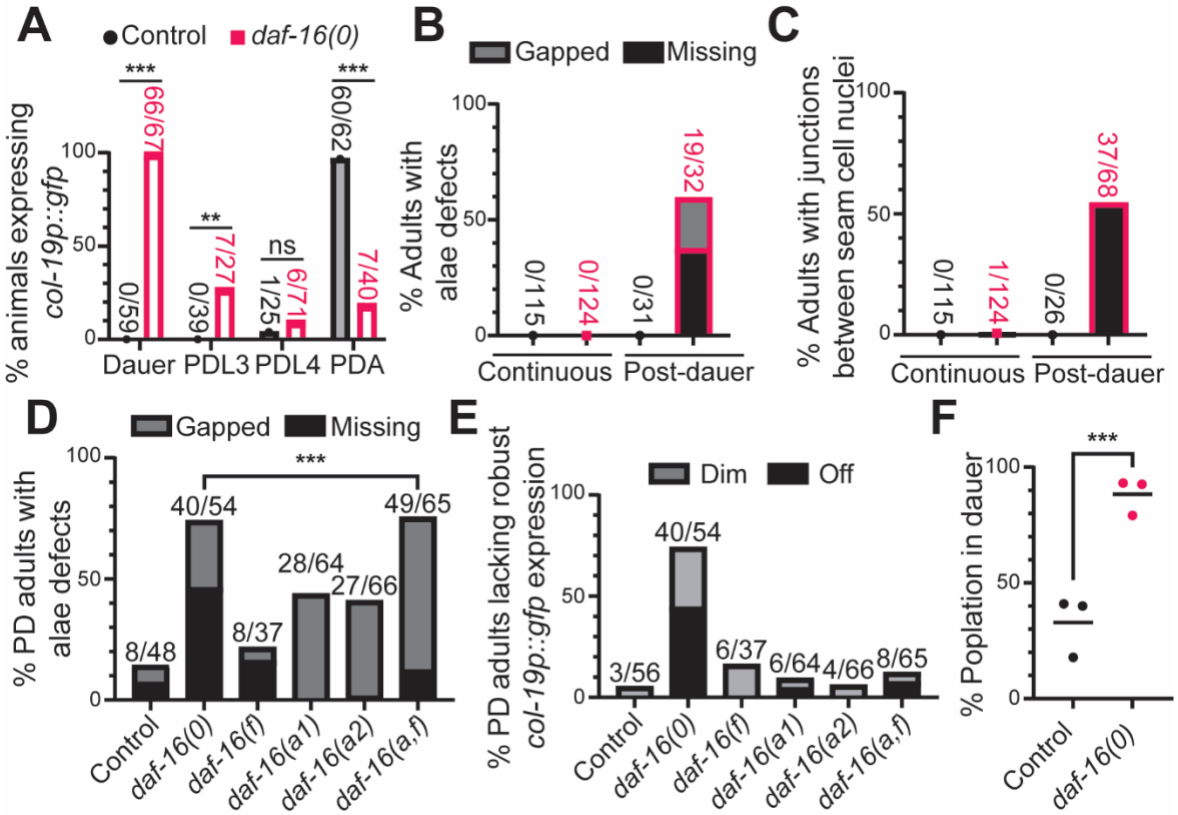

Figure 1. *daf-16* coordinates the exit from dauer and the resumption of seam cell development after dauer. (A) The penetrance of *daf-16(0)* animals expressing *col-19p::gfp* remains low in all post-dauer (PD) stages, including in adults. **p=0.0011, ***p<0.001, 2X3 Fisher's exact test, two tailed. (B) *daf-16(0)* PD adults had defects in adult alae synthesis. In B and subsequent figures showing adult alae, numbers indicate the number of adults with defects, defined as missing or gapped alae, over the total number of adults assessed. (C) *daf-16(0)* PD adults had junctions present between seam cells. Adults were counted as having junctions if at least one junction was observed between seam cells. We observed animals with anywhere from 1-6 junctions. We also found that 18/68 *daf-16(0)* and 2/26 control PD adults showed evidence of seam cell division (Podbilewicz and White 1994). (D) All major *daf-16* isoforms contribute to the expression of adult alae after dauer. *daf-16(a1)* and *daf-16(a2)* are two independent mutations that delete the *daf-16(a)* isoform (Chen et al. 2015). The *daf-16(a,f)* mutant had less severe defects in adult alae compared to the *daf-16(0)* PD adults. ***p<0.001, 2X3 Fisher's exact test, two-tailed. (E) All major *daf-16* isoforms contribute to the expression of *col-19p::gfp* after dauer. (F) *daf-16(0)* larvae recover poorly from dauer. Each data point represents the

population of larvae remaining in dauer 24 hours after shifting dauer larvae from 24°C to 20°C in an individual experiment (n=20-29 larvae per data point). ***$p<0.001$, 2X2 Fisher's exact test, one-tailed.

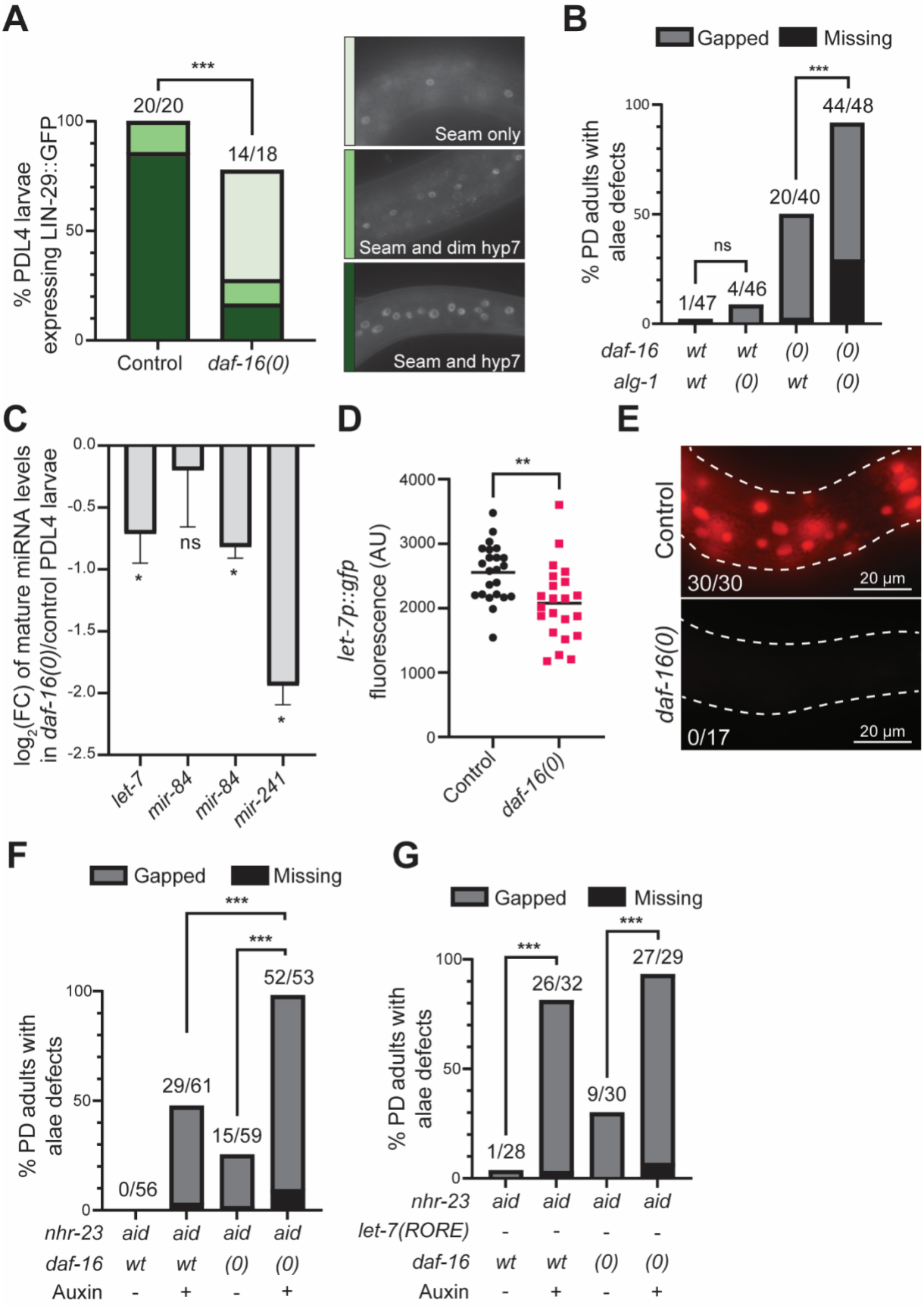
A
% PDL4 larvae expressing LIN-29::GFP
100
50
0
***
20/20
14/18
Control
daf-16(0)
Seam only
Seam and dim hyp7
Seam and hyp7
B
Gapped
Missing
% PD adults with alae defects
100
50
0
***
44/48
20/40
ns
1/47
4/46
daf-16 wt wt (0) (0)
alg-1 wt (0) wt (0)
C
log2(FC) of mature miRNA levels in daf-16(0)/control PDL4 larvae
0.0
-0.5
-1.0
-1.5
-2.0
-2.5
*
ns
*
*
let-7
mir-84
mir-84
mir-241
D
let-7p::gfp fluorescence (AU)
4000
3000
2000
1000
0
**
Control
daf-16(0)
E
Control
30/30
20 µm
daf-16(0)
0/17
20 µm
F
Gapped
Missing
% PD adults with alae defects
100
50
0
***
***
52/53
29/61
15/59
0/56
nhr-23 aid aid aid aid
daf-16 wt wt (0) (0)
Auxin - + - +
G
Gapped
Missing
% PD adults with alae defects
100
50
0
***
***
27/29
26/32
9/30
1/28
nhr-23 aid aid aid aid
let-7(RORE) - - - -
daf-16 wt wt (0) (0)
Auxin - + - +

Figure 2. *daf-16* promotes the expression of heterochronic genes. (A) *daf-16(0)* PDL4 larvae expressed LIN-29::GFP in fewer hypodermal nuclei than control larvae. ***p<0.001, 2X3 Fisher's exact test, two-tailed. Representative images of LIN-29::GFP expression patterns used to bin larvae are shown. Numbers indicate the number of larvae expressing LIN-29::GFP at any detectable level out of total number scored. (B) *daf-16(0)* and *alg-1(0)* alleles showed mutual enhancement for defects in adult alae after dauer. ***p<0.001, 2X3 Fisher's exact test, two-tailed. (C) *daf-16(0)* PDL4 larvae expressed reduced levels of mature *let-7* family microRNAs. miRNA reads were normalized to U18. *p<0.05, T-Test, two-tailed. (D) *daf-16(0)* PDL4 larvae expressed reduced levels of *let-7p::gfp*. Each data point represents the expression of *let-7p::gfp* throughout the body of one PDL4 larva. **p=0.0015, Mann-Whitney test, two-tailed. (E) *daf-16(0)* PDL3m larvae showed greatly reduced expression of an endogenous *mir-241* transcriptional reporter. Numbers indicate the number of PDL3m larvae with robust *mir-241p::mScarlet* expression over total number of larvae assessed. White dashed lines show the outline of the worm. (F) *daf-16(0)* and *nhr-23(aid)* alleles showed mutual enhancement in adult alae defects after dauer. ***p<0.001, 2X3 Fisher's exact test, two-tailed. (G) *let-7* mutants with the NHR-23 binding sites disrupted did not phenocopy the defects in adult alae seen in *nhr-23(aid)* mutants after dauer. ***p<0.001, 2X3 Fisher's exact test, two-tailed.

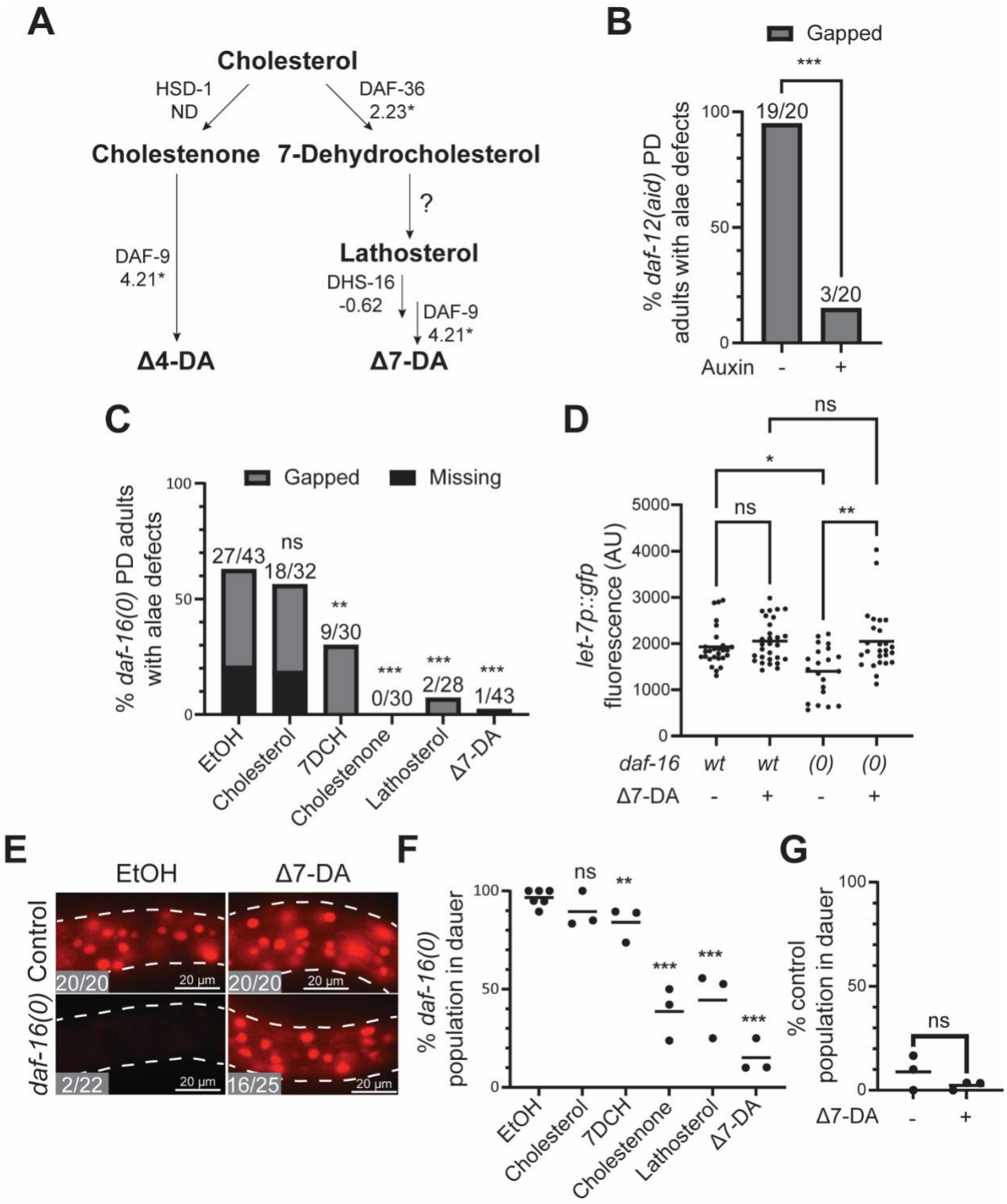

Figure 3. *daf-16* promotes the production of dafachronic acid to regulate adult cell fate. (A) Model of the biosynthetic pathway for the two originally described forms of DA, Δ4-DA and Δ7-DA (Motola et al. 2006) . Model adapted from Aguilaniu et al. (2021). Chemical compounds

are highlighted in bold and the enzymes that catalyze each reaction are listed. Numbers below enzyme names indicate the $\log_2$(Fold change) in expression of each gene in *daf-16(0); daf-7* vs *daf-7* dauer larvae, from Wirick et al. (2021). Asterisks indicate that the change in gene expression was statistically significant (FDR < 0.05). ND = Not detected in either sample. (B) The *daf-12(aid)* allele had penetrant defects in alae formation which are suppressed when DAF-12 is depleted. ***p<0.001, 2X2 Fisher's exact test, one-tailed. (C) Treatment of 100nM Δ7-DA or 33.3μM of intermediates downstream of cholesterol suppressed alae defects in *daf-16(0)* PD adults, while treatment with 33.3μM cholesterol appeared similar to the control EtOH carrier. **p=0.003, ***p<0.001, 2X3 Fisher's exact test, two-tailed. (D) Treatment of 100nM Δ7-DA restored *let-7p::gfp* expression in *daf-16(0)* PDL4 larvae. Each data point represents the whole body expression of *let-7p::gfp* for one PDL4 larva. *p=0.029, **p<0.01, Kruskal-Wallis test with Dunn's multiple comparisons test. (E) Treatment of Δ7-DA restored robust *mir-241p::mScarlet* expression in *daf-16(0)* PDL3m larvae. Numbers indicate the number of PDL3m larvae with robust *mir-241p::mScarlet* expression over total number of larvae assessed. White dashed lines outline worm cuticles. (F) Treatment of 100nM Δ7-DA or 33.3μM of intermediates downstream of cholesterol suppressed dauer recovery defects in *daf-16(0)* PD adults, whereas 33.3μM cholesterol did not (n=16-21 larvae per data point). **p=0.006, ***p<0.001, 2X2 Fisher's exact test, one-tailed. (G) Treatment of Δ7-DA did not enhance dauer recovery in control animals (n=24-30 larvae per data point). p=0.083, 2X2 Fisher's exact test, one-tailed. (F-G) Each data point represents the population of animals that remained in dauer 24 hours after shifting dauer larvae from 24°C to 20°C in an individual experiment.

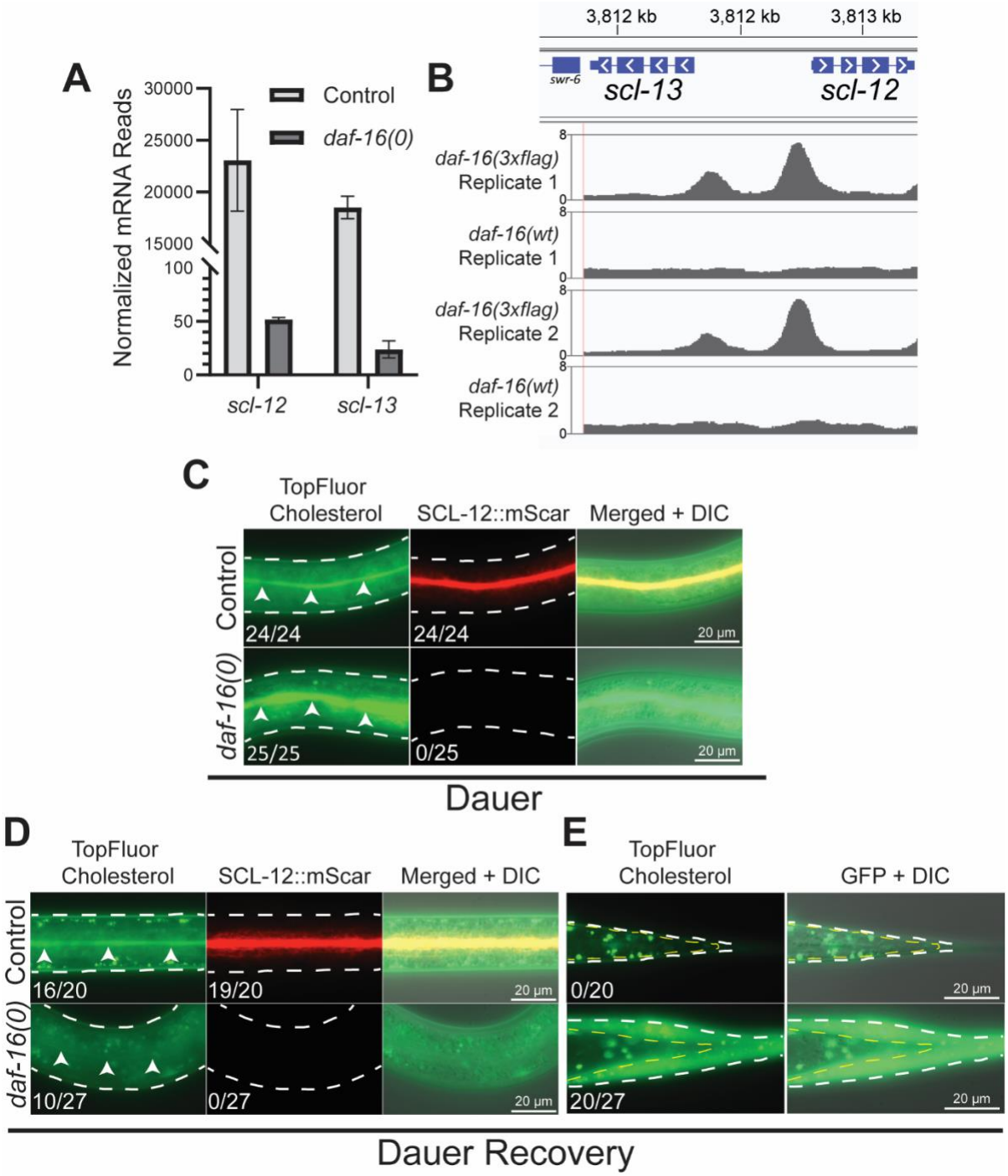

Figure 4. *daf-16* promotes the retention of intestinal cholesterol upon dauer recovery. (A) *daf-16* promotes the expression of *scl-12* and *scl-13*. Normalized mRNA reads in control and *daf-16(0)* dauer larvae, from Wirick et al. (2021). Error bars denote the standard deviation between two biological replicates. (B) DAF-16 binds upstream of *scl-12* and *scl-13*. DAF-16::3xflag binding peaks in two *daf-16(3xflag)* and two *daf-16(wt)* (N2) replicates. Kilobases

represent the relative location on chromosome V. White arrowheads represent the direction of transcription. (C) *daf-16(0)* dauer larvae sequestered TopFluor cholesterol but lack SCL-12::mScarlet expression in the intestinal lumen. (D) *daf-16(0)* larvae recovering from dauer lacked TopFluor cholesterol and SCL-12::mScarlet expression in the intestinal lumen. (E) TopFluor cholesterol in *daf-16(0)* larvae recovering from dauer localized between the epidermis and the cuticle. (D-E) Dauer recovery was induced with 100nM Δ7-DA. Images were taken 7 hours after administration of Δ7-DA. (B-E) White dashed lines outline worm cuticles. In (E), there was a gap between the worm body and a cuticle; the worm body is indicated with dashed yellow lines. Numbers represent the number of larvae with detectable expression of TopFluor cholesterol or SCL-12::mScarlet over total number of larvae assessed. (C-D) White arrow head point to the intestinal lumen.

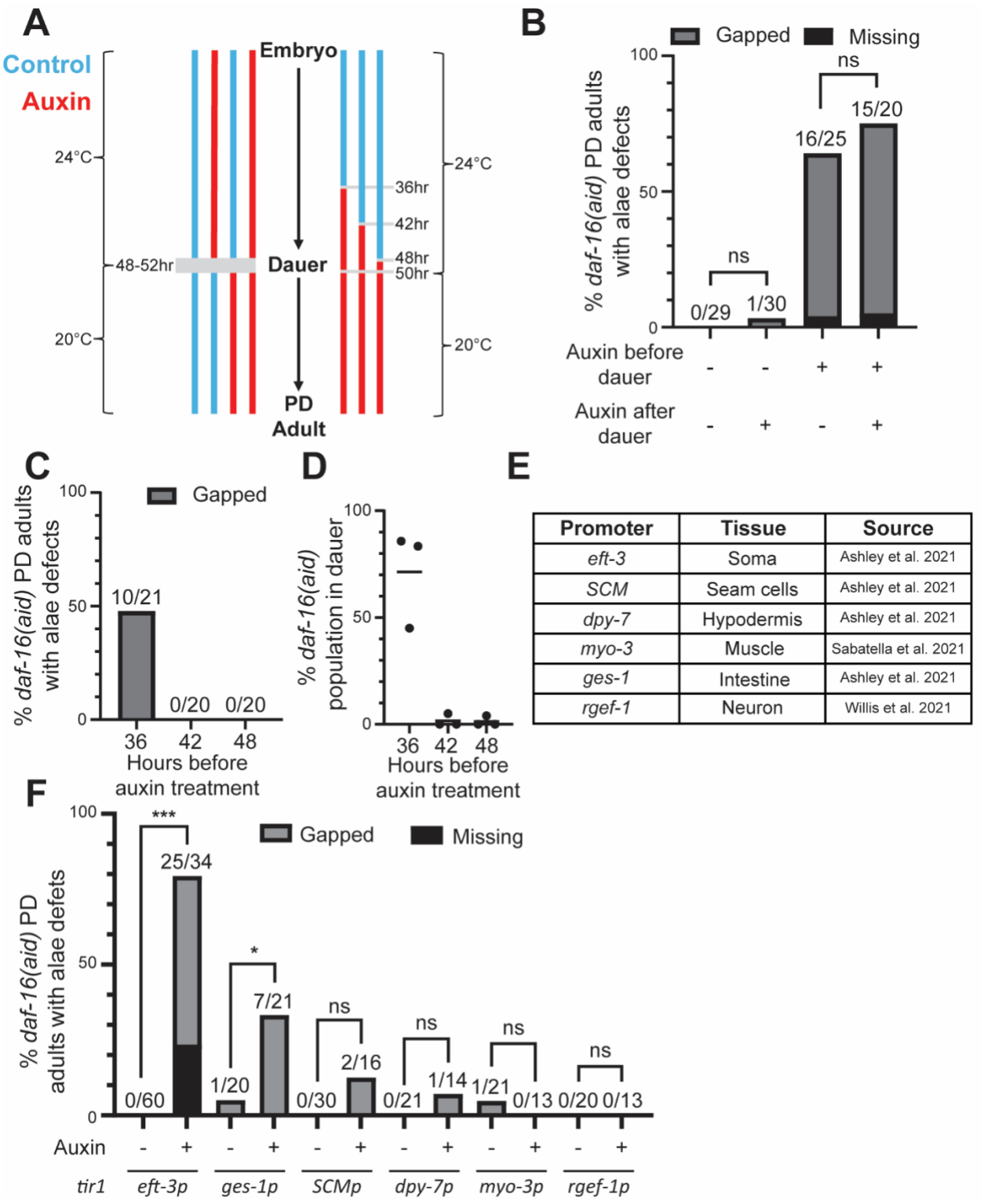

Promoter	Tissue	Source
eft-3	Soma	Ashley et al. 2021
SCM	Seam cells	Ashley et al. 2021
dpy-7	Hypodermis	Ashley et al. 2021
myo-3	Muscle	Sabatella et al. 2021
ges-1	Intestine	Ashley et al. 2021
rgef-1	Neuron	Willis et al. 2021

Figure 5. DAF-16 functions before dauer in the intestine to promote adult cell fate after dauer. (A) Model for auxin treatments in B-D, where time 0 = the time when embryos were semi-synchronized by sodium hypochlorite treatment. The left side refers to data shown in panel

B, where dauer larvae were shifted from 24°C to 20°C 48-52 hours after embryo synchronization. The right refers to data shown in panels C-D, where dauer larvae were shifted from 24°C to 20°C 50 hours after synchronization. Blue bars indicate times that larvae were on NGM plates and red bars indicate times on auxin plates. Gray bars represent time points that larvae were passed to a new plate. Dauer formation occurs approximately at 48 hours (B) Somatic depletion of DAF-16 before dauer resulted in defects in adult alae after dauer. (C-D) DAF-16 is required between 12 and 6 hours before dauer formation to promote the expression of adult alae after dauer. Somatic depletion of DAF-16 12 hours before dauer entry (36 h after synchronization) resulted in defects in adult alae after dauer (C) and dauer recovery (D). (D) Each data point represents the population of animals remaining in dauer 24 hours after shifting dauer larvae from 24°C to 20°C in an individual experiment (n=18-25 larvae per data point). (E) Table of tissue specific *tir1* drivers including promoter, tissue that expression is expected in, and source of the transgene (Ashley et al. 2021; Sabatella et al. 2021; Willis et al. 2021). (F) Depletion of DAF-16 in intestinal tissue resulted in adult alae defects after dauer. ***$p<0.001$, *$p=0.044$, 2X3 Fisher's exact test, two-tailed.

References

Abbott AL, Alvarez-Saavedra E, Miska EA, Lau NC, Bartel DP, Horvitz HR, Ambros V. 2005. The *let-7* microRNA family members *mir-48, mir-84,* and *mir-241* function together to regulate developmental timing in *Caenorhabditis elegans*. Developmental Cell. 9(3):403–414. doi:10.1016/j.devcel.2005.07.009.

Abrahante JE, Daul AL, Li M, Volk ML, Tennessen JM, Miller EA, Rougvie AE. 2003. The *Caenorhabditis elegans* hunchback-like gene *lin-57/hbl-1* controls developmental time and is regulated by microRNAs. Developmental Cell. 4(5):625–637.

Aeschimann F, Neagu A, Rausch M, Großhans H. 2019. *let-7* coordinates the transition to adulthood through a single primary and four secondary targets. Life Sci Alliance. 2(2):e201900335. doi:10.26508/lsa.201900335.

Aguilaniu H, Fabrizio P, Witting M. 2016. The Role of Dafachronic Acid Signaling in Development and longevity in *Caenorhabditis elegans*: Digging deeper using cutting-edge analytical chemistry. Front Endocrinol. 7:12. doi:10.3389/fendo.2016.00012.

Ambros V. 1989. A hierarchy of regulatory genes controls a larva-to-adult developmental switch in *C. elegans*. Cell. 57(1):49–57. doi:10.1016/0092-8674(89)90171-2.

Ambros V, Horvitz H. 1984. Heterochronic mutants of the nematode *Caenorhabditis elegans*. Science. 226(4673):409–416. doi:10.1126/science.6494891.

Antebi A, Culotti JG, Hedgecock EM. 1998. *daf-12* regulates developmental age and the dauer alternative in *Caenorhabditis elegans*. Development. 125(7):1191–1205.

Antebi A, Yeh WH, Tait D, Hedgecock EM, Riddle DL. 2000. *daf-12* encodes a nuclear receptor that regulates the dauer diapause and developmental age in *C. elegans*. Genes & Development. 14(12):1512–1527. doi:10.1101/gad.14.12.1512.

Ashley GE, Duong T, Levenson MT, Martinez MAQ, Johnson LC, Hibshman JD, Saeger HN, Palmisano NJ, Doonan R, Martinez-Mendez R, et al. 2021. An expanded auxin-inducible degron toolkit for *Caenorhabditis elegans*. Genetics. 217(3):iyab006. doi:10.1093/genetics/iyab006.

Azzi C, Aeschimann F, Neagu A, Großhans H. 2020. A branched heterochronic pathway directs juvenile-to-adult transition through two LIN-29 isoforms. Elife. 9:e53387. doi:10.7554/elife.53387.

Baugh LR, Hu PJ. 2020. Starvation Responses Throughout the *Caenorhabditis elegans* Life Cycle. Genetics. 216(4):837–878. doi:10.1534/genetics.120.303565.

Bethke A, Fielenbach N, Wang Z, Mangelsdorf DJ, Antebi A. 2009. Nuclear hormone receptor regulation of microRNAs controls developmental progression. Science. 324(5923):95–98. doi:10.1126/science.1164899.

Bettinger JC, Lee K, Rougvie AE. 1996. Stage-specific accumulation of the terminal differentiation factor LIN-29 during *Caenorhabditis elegans* development. Development. 122(8):2517–2527.

Billi AC, Alessi AF, Khivansara V, Han T, Freeberg M, Mitani S, Kim JK. 2012. The *Caenorhabditis elegans* HEN1 ortholog, HENN-1, methylates and stabilizes select subclasses of germline small RNAs. PLoS Genet. 8(4):e1002617. doi:10.1371/journal.pgen.1002617.

Brenner S. 1974. The genetics of *Caenorhabditis elegans*. Genetics. 77(1):71–94. doi:10.1093/genetics/77.1.71.

Cale AR, Karp X. 2020. *lin-41* controls dauer formation and morphology via *lin-29 in C. elegans*. Micropublication Biology. 2020:10.17912/micropub.biology.000323. doi:10.17912/micropub.biology.000323.

Cassada RC, Russell RL. 1975. The dauerlarva, a post-embryonic developmental variant of the nematode *Caenorhabditis elegans*. Dev Biol. 46(2):326–342. doi:10.1016/0012-1606(75)90109-8.

Chalfie M, Horvitz HR, Sulston JE. 1981. Mutations that lead to reiterations in the cell lineages of *C. elegans*. Cell. 24(1):59–69.

Chen AT-Y, Guo C, Itani OA, Budaitis BG, Williams TW, Hopkins CE, McEachin RC, Pande M, Grant AR, Yoshina S, et al. 2015. Longevity genes revealed by integrative analysis of isoform-

specific *daf-16/FoxO* mutants of *Caenorhabditis elegans*. Genetics. 201(2):613–629. doi:10.1534/genetics.115.177998.

Chen D, Riddle DL. 2008. Function of the PHA-4/FOXA transcription factor during *C. elegans* post-embryonic development. BMC Developmental Biology. 8(1):26. doi:10.1186/1471-213x-8-26.

Chitwood DJ. 1997. Biochemistry and function of nematode sterols. :169–180. doi:10.1201/9781003068754-12.

Fay DS, Stanley HM, Han M, Wood WB. 1999. A *Caenorhabditis elegans* homologue of hunchback is required for late stages of development but not early embryonic patterning. Developmental Biology. 205(2):240–253. doi:10.1006/dbio.1998.9096.

Fielenbach N, Antebi A. 2008. *C. elegans* dauer formation and the molecular basis of plasticity. Genes & Development. 22(16):2149–2165. doi:10.1101/gad.1701508.

Gerisch B, Antebi A. 2004. Hormonal signals produced by DAF-9/cytochrome P450 regulate *C. elegans* dauer diapause in response to environmental cues. Development. 131(8):1765–1776. doi:10.1242/dev.01068.

Gerisch B, Weitzel C, Kober-Eisermann C, Rottiers V, Antebi A. 2001. A hormonal signaling pathway influencing *C. elegans* metabolism, reproductive development, and life span. Developmental Cell. 1(6):841–851.

Gerstein MB, Lu ZJ, Nostrand ELV, Cheng C, Arshinoff BI, Liu T, Yip KY, Robilotto R, Rechtsteiner A, Ikegami K, et al. 2010. Integrative analysis of the *Caenorhabditis elegans* genome by the modENCODE project. Science. 330(6012):1775–1787. doi:10.1126/science.1196914.

Hammell CM, Karp X, Ambros V. 2009. A feedback circuit involving *let-7*-family miRNAs and DAF-12 integrates environmental signals and developmental timing in *Caenorhabditis elegans*. Proceedings of the National Academy of Sciences. 106(44):18668–18673. doi:10.1073/pnas.0908131106.

Hand SC, Denlinger DL, Podrabsky JE, Roy R. 2016. Mechanisms of animal diapause: recent developments from nematodes, crustaceans, insects, and fish. Am J Physiology-regulatory Integr Comp Physiology. 310(11):R1193–R1211. doi:10.1152/ajpregu.00250.2015.

Hansen MA, Dahal A, Bernstein TA, Kohtz C, Ali S, Daul AL, Montoye E, Panzade GP, Alessi AF, Flibotte S, et al. 2022. *ztf-16* is a novel heterochronic modulator that opposes adult cell fate in dauer and continuous life histories in *Caenorhabditis elegans*. bioRxiv.:2022.06.20.496913. doi:10.1101/2022.06.20.496913.

Hayes GD, Frand AR, Ruvkun G. 2006. The *mir-84* and *let-7* paralogous microRNA genes of *Caenorhabditis elegans* direct the cessation of molting via the conserved nuclear hormone receptors NHR-23 and NHR-25. Development. 133(23):4631–4641. doi:10.1242/dev.02655.

Hong Y, Roy R, Ambros V. 1998. Developmental regulation of a cyclin-dependent kinase inhibitor controls postembryonic cell cycle progression in *Caenorhabditis elegans*. Development. 125(18):3585–3597.

Ilbay O, Ambros V. 2019. Pheromones and nutritional signals regulate the developmental reliance on *let-7* family microRNAs in *C. elegans*. Curr Biol. doi:10.1016/j.cub.2019.04.034.

Jackson BM, Abete-Luzi P, Krause MW, Eisenmann DM. 2014. Use of an activated Beta-catenin to identify wnt pathway target genes in *Caenorhabditis elegans*, including a subset of collagen genes expressed in late larval development. G3: Genes, Genomes, Genet. 4(4):733–747. doi:10.1534/g3.113.009522.

Johnson LC, Vo AA, Clancy JC, Myles KM, Pooranachithra M, Aguilera J, Levenson MT, Wohlenberg C, Rechtsteiner A, Ragle JM, et al. 2023. NHR-23 activity is necessary for *C. elegans* developmental progression and apical extracellular matrix structure and function. Development. doi:10.1242/dev.201085.

Kamath RS, Ahringer J. 2003. Genome-wide RNAi screening in *Caenorhabditis elegans*. Methods. 30(4):313–321. doi:10.1016/s1046-2023(03)00050-1.

Karp X. 2018. Working with dauer larvae. WormBook. 2018:1–19. doi:10.1895/wormbook.1.180.1.

Karp X. 2021. Hormonal regulation of diapause and development in nematodes, insects, and fishes. Frontiers Ecol Evol. 09:735924. doi:10.3389/fevo.2021.735924.

Karp X, Ambros V. 2011. The developmental timing regulator *hbl-1* modulates the dauer formation decision in *Caenorhabditis elegans*. Genetics. 187(1):345–353. doi:10.1534/genetics.110.123992.

Karp X, Ambros V. 2012. Dauer larva quiescence alters the circuitry of microRNA pathways regulating cell fate progression in *C. elegans*. Development. 139(12):2177–2186. doi:10.1242/dev.075986.

Kouns NA, Nakielna J, Behensky F, Krause MW, Kostrouch Z, Kostrouchova M. 2011. NHR-23 dependent collagen and hedgehog-related genes required for molting. Biochem Biophys Res Commun. 413(4):515–520. doi:10.1016/j.bbrc.2011.08.124.

Lin SY, Johnson SM, Abraham M, Vella MC, Pasquinelli A, Gamberi C, Gottlieb E, Slack FJ. 2003. The *C elegans* hunchback homolog, *hbl-1*, controls temporal patterning and is a probable microRNA target. Developmental Cell. 4(5):639–650.

Liu Z, Ambros V. 1991. Alternative temporal control systems for hypodermal cell differentiation in *Caenorhabditis elegans*. Nature. 350(6314):162–165. doi:10.1038/350162a0.

Liu Z, Kirch S, Ambros V. 1995. The *Caenorhabditis elegans* heterochronic gene pathway controls stage-specific transcription of collagen genes. Dev Camb Engl. 121(8):2471–8.

Ludewig AH, Kober-Eisermann C, Weitzel C, Bethke A, Neubert K, Gerisch B, Hutter H, Antebi A. 2004. A novel nuclear receptor/coregulator complex controls *C. elegans* lipid metabolism, larval development, and aging. Genes & Development. 18(17):2120–2133. doi:10.1101/gad.312604.

Mak HY, Ruvkun G. 2004. Intercellular signaling of reproductive development by the *C. elegans* DAF-9 cytochrome P450. Development. 131(8):1777–1786. doi:10.1242/dev.01069.

Motola DL, Cummins CL, Rottiers V, Sharma KK, Li T, Li Y, Suino-Powell K, Xu HE, Auchus RJ, Antebi A, et al. 2006. Identification of ligands for DAF-12 that govern dauer formation and reproduction in *C. elegans*. Cell. 124(6):1209–1223. doi:10.1016/j.cell.2006.01.037.

Nika L, Gibson T, Konkus R, Karp X. 2016. Fluorescent beads are a versatile tool for staging *Caenorhabditis elegans* in different life histories. G3 Genes Genomes Genetics. 6(7):1923–1933. doi:10.1534/g3.116.030163.

Nolan T, Hands RE, Bustin SA. 2006. Quantification of mRNA using real-time RT-PCR. Nat Protoc. 1(3):1559–1582. doi:10.1038/nprot.2006.236.

Ogg S, Paradis S, Gottlieb S, Patterson GI, Lee L, Tissenbaum HA, Ruvkun G. 1997. The Fork head transcription factor DAF-16 transduces insulin-like metabolic and longevity signals in *C. elegans*. Nature. 389(6654):994–999. doi:10.1038/40194.

Ogg S, Ruvkun G. 1998. The *C. elegans* PTEN homolog, DAF-18, acts in the insulin receptor-like metabolic signaling pathway. Molecular Cell. 2(6):887–893.

Patel R, Galagali H, Kim JK, Frand AR. 2022. Feedback between a retinoid-related nuclear receptor and the *let-7* microRNAs controls the pace and number of molting cycles in *C. elegans*. Elife. 11:e80010. doi:10.7554/elife.80010.

Podbilewicz B, White JG. 1994. Cell fusions in the developing epithelia of *C. elegans*. Dev Biol. 161(2):408–424. doi:10.1006/dbio.1994.1041.

Reinhart BJ, Slack FJ, Basson M, Pasquinelli AE, Bettinger JC, Rougvie AE, Horvitz HR, Ruvkun G. 2000. The 21-nucleotide *let-7* RNA regulates developmental timing in *Caenorhabditis elegans*. Nature. 403(6772):901–906. doi:10.1038/35002607.

Rougvie AE, Ambros V. 1995. The heterochronic gene *lin-29* encodes a zinc finger protein that controls a terminal differentiation event in *Caenorhabditis elegans*. Development. 121(8):2491–2500.

Rougvie AE, Moss EG. 2013. Developmental transitions in *C. elegans* larval stages. Current topics in developmental biology. 105:153–180. doi:10.1016/b978-0-12-396968-2.00006-3.

Sabatella M, Thijssen KL, Davó-Martínez C, Vermeulen W, Lans H. 2021. Tissue-specific DNA repair activity of ERCC-1/XPF-1. Cell Rep. 34(2):108608. doi:10.1016/j.celrep.2020.108608.

Schmeisser K, Kaptan D, Raghuraman BK, Shevchenko A, Rodenfels J, Penkov S, Kurzchalia TV. 2024. Mobilization of cholesterol induces the transition from quiescence to growth in

Caenorhabditis elegans through steroid hormone and mTOR signaling. Commun Biol. 7(1):121. doi:10.1038/s42003-024-05804-7.

Slack FJ, Basson M, Liu Z, Ambros V, Horvitz HR, Ruvkun G. 2000. The *lin-41* RBCC gene acts in the *C. elegans* heterochronic pathway between the *let-7* regulatory RNA and the LIN-29 transcription factor. Mol Cell. 5(4):659–669. doi:10.1016/s1097-2765(00)80245-2.

Sulston JE, Horvitz HR. 1977. Post-embryonic cell lineages of the nematode, *Caenorhabditis elegans*. Dev Biol. 56(1):110–156. doi:10.1016/0012-1606(77)90158-0.

Sun S, Ohta A, Kuhara A, Nishikawa Y, Kage-Nakadai E. 2019. *daf-16/FOXO* isoform *b* in AIY neurons is involved in low preference for *Bifidobacterium infantis* in *Caenorhabditis elegans*. Neuroscience research. doi:10.1016/j.neures.2019.01.011.

Sym M, Basson M, Johnson C. 2000. A model for Niemann–Pick type C disease in the nematode *Caenorhabditis elegans*. Curr Biol. 10(9):527–530. doi:10.1016/s0960-9822(00)00468-1.

Tennessen JM, Opperman KJ, Rougvie AE. 2010. The *C. elegans* developmental timing protein LIN-42 regulates diapause in response to environmental cues. Development. 137(20):3501–3511. doi:10.1242/dev.048850.

Timmons L, Fire A. 1998. Specific interference by ingested dsRNA. Nature. 395(6705):854. doi:10.1038/27579.

Vowels JJ, Thomas JH. 1992. Genetic analysis of chemosensory control of dauer formation in *Caenorhabditis elegans*. Genetics. 130(1):105–123.

Willis AR, Zhao W, Sukhdeo R, Wadi L, Jarkass HTE, Claycomb JM, Reinke AW. 2021. A parental transcriptional response to *microsporidia* infection induces inherited immunity in offspring. Sci Adv. 7(19):eabf3114. doi:10.1126/sciadv.abf3114.

Wirick MJ, Cale AR, Smith IT, Alessi AF, Starostik MR, Cuko L, Lalk K, Schmidt MN, Olson BS, Salomon PM, et al. 2021. *daf-16/FOXO* blocks adult cell fate in *Caenorhabditis elegans* dauer larvae via *lin-41/TRIM71*. Plos Genet. 17(11):e1009881. doi:10.1371/journal.pgen.1009881.

Zhang L, Ward JD, Cheng Z, Dernburg AF. 2015. The auxin-inducible degradation (AID) system enables versatile conditional protein depletion in *C. elegans*. Development. 142(24):4374–4384. doi:10.1242/dev.129635.

Zhang MG, Sternberg PW. 2022. Both entry to and exit from diapause arrest in *Caenorhabditis elegans* are regulated by a steroid hormone pathway. Development. 149(9):dev200173. doi:10.1242/dev.200173.